Supplementary Materials for

Tissue-of-origin Dictates Branched-Chain Amino Acid Metabolism in Mutant *Kras*-driven Cancers

Jared R. Mayers[1,2*], Margaret E. Torrence[1,2*], Laura V. Danai[1], Thales Papagiannakopoulos[1†], Shawn M. Davidson[1,2], Matthew R. Bauer[1], Allison N. Lau[1], Brian W. Ji[3], Purushottam D. Dixit[3], Aaron M. Hosios[1,2], Alexander Muir[1], Christopher R. Chin[1], Elizaveta Freinkman[1,2,4,5,6], Tyler Jacks[1,2,6], Brian M. Wolpin[7], Dennis Vitkup[3], and Matthew G. Vander Heiden[1,2,5,7,‡]

Affiliations:
[1]Koch Institute for Integrative Cancer Research, Massachusetts Institute of Technology, Cambridge, Massachusetts 02139, USA.
[2]Department of Biology, Massachusetts Institute of Technology, Cambridge, Massachusetts 02139, USA.
[3]Center for Computational Biology and Bioinformatics and Initiative in Systems Biology, Columbia University, New York, New York 10027, USA.
[4]Whitehead Institute for Biomedical Research, Nine Cambridge Center, Cambridge, Massachusetts 02142, USA.
[5]Broad Institute, Seven Cambridge Center, Cambridge, Massachusetts 02142, USA.
[6]Howard Hughes Medical Institute, Massachusetts Institute of Technology, Cambridge, Massachusetts 02139, USA.
[7]Dana-Farber Cancer Institute, Boston, Massachusetts 02115, USA.
*Equal contribution
[†]Current Address: School of Medicine, New York University, New York, New York 10016, USA

correspondence to: Matthew G. Vander Heiden, mvh@mit.edu

This PDF file includes:

Materials and Methods

Experimental Mice

All studies were approved by the MIT committee on animal care (IACUC). All experimental groups were assigned based on genotype. All animals were numbered and experiments conducted blinded. After data collection genotypes were revealed and animals assigned to groups for analysis.

KPC: Experimental KPC mice were male mice on a pure C57BL/6J background. Experimental mice were heterozygous for the conditional lox–stop–lox $Kras^{G12D}$ allele, heterozygous for the conditional lox–stop–lox $Trp53^{R172H}$ allele and expressed Cre–recombinase under control of the Pdx–1–promoter ($Tg(Ipf1\text{-}cre)1^{Tuv}$) (*26*). Littermate controls lacked either the LSL–$Kras^{G12D}$ allele, the Cre allele, or both. Control mice were sacrificed at the same time as their tumor–bearing littermates.

$KP^{-/-}C$ (PDAC): Experimental $KP^{-/-}C$ mice were male mice on a pure C57BL/6J background. Experimental mice were heterozygous for the conditional lox–stop–lox $Kras^{G12D}$ allele, homozygous for loxP sites flanking exons 2–10 of *Trp53* and expressed Cre–recombinase under control of the Pdx–1–promoter ($Tg(Ipf1\text{-}cre)1^{Tuv}$) (*19*). Littermate control mice lacked either the Cre–recombinase allele, *LSL–*$Kras^{G12D}$ allele, or both as previously described (*18*), such that control pancreas samples used throughout were derived from a combination of p53 wildtype and null pancreata. Cancer cell lines derived from these mice were used for syngenic implantation studies. For FACS sorting, mixed background male mice with the $KP^{-/-}C$ alleles plus a *LSL-tdTomato* reporter gene expressed under control of the Rosa-26 promoter ($Gt(ROSA)^{26Sor\ tm9(CAG\text{-}tdTomato)Hze}$/+) were used. Five-week old mice were used for the experiment presented in fig. S1, whereas 8-10-week-old mice were used for all other experiments presented in the study.

KP Non–small cell lung cancer: Experimental NSCLC mice were male mice on a pure C57BL/6J background. Experimental mice were heterozygous for the conditional lox–stop–lox $Kras^{G12D}$ allele, homozygous for loxP sites flanking exons 2–10 of *Trp53* were administered $2.5x10^7$ pfu of Cre–expressing adenovirus intratracheally as previously described (*20*). Control mice lacked the lox–stop–lox $Kras^{G12D}$ allele, but contained the floxed-*Trp53* allele. High–titer adenovirus was obtained from the Gene Transfer Vector Core (University of Iowa). Cre was administered when the mice were 8-12 weeks of age. Cancer cell lines derived from these mice were used for syngenic implantation studies. Mice 8-weeks post-infection were used for the experiment presented in fig. S1, whereas mice 12-14-weeks post-infection were used for all other experiments presented in the study.

Subcutaneous and orthotopic implantation studies: Male C57BL/6J mice aged 6-12 weeks at the start of the study were used for these experiments.

Diets

Standard Chow Diet: RMH 3000 (Prolab).

Amino Acid Defined Diet: Control (unlabeled) amino acid-defined diet (TD.110839) was designed in consultation with and subsequently obtained from Harlan Teklad.

^{13}C-BCAA Amino Acid Defined Diet: 20% ^{13}C–leucine and 20% ^{13}C–valine labeled diet was based on diet TD.110839 and produced by Cambridge Isotopes and Harlan Teklad. $KP^{-/-}C$ PDAC mice and NSCLC mice were fed this diet for 7 days beginning at seven weeks of age (PDAC) and 12-weeks post infection with adenoviral Cre-recombinase (NSCLC).

^{15}N-Leu Amino Acid Defined Diet: 50% ^{15}N–leucine labeled diet was based on diet TD.110839 and produced by Cambridge Isotopes and Harlan Teklad. KP$^{-/-}$C PDAC mice were fed this diet for 7 days beginning at seven weeks of age (PDAC). NSCLC mice were fed this diet for 6 days, beginning 12-weeks post infection with adenoviral Cre-recombinase (NSCLC).

Plasma Collection

Mice were anesthetized under 2% isofluorane–oxygen mixture and retro–orbitally bled approximately 4.5 hours after the onset of the light cycle. Blood was immediately placed in EDTA-tubes and centrifuged to separate plasma. Plasma was aliquoted and frozen at -80˚C for further analysis.

LC–MS Plasma Amino Acid Measurements

Plasma amino acids were measured by LC–MS at the Koch Institute at the Massachusetts Institute of Technology (Cambridge, MA) using methods previously described (*18*). Raw data were analyzed as peak area tops using the open–access MAVEN software tool (*40*).

GC–MS Assessment of Stable Isotope Labeling

Plasma polar metabolites were extracted in ice–cold 4:1 methanol:water with norvaline internal standard (5µL plasma in 200µL extraction solution). Extracts were clarified by centrifugation and the supernatant evaporated under nitrogen and frozen at –80˚C for subsequent derivitization. Dried polar metabolites were dissolved in 20µL of 2% methoxyamine hydrochloride in pyridine (Thermo) and held at 37˚C for 1.5hr. After dissolution and reaction, tert–butyldimethylsilyl derivatization was initiated by adding 25µL *N*–methyl–*N*–(tert–butyldimethylsilyl)trifluoroacetamide + 1% tert–butyldimethylchlorosilane (Sigma) and incubating at 37˚C for 1hr.

All tissues used for metabolomic analysis were snap frozen using a BioSpec Biosquezer (#1210). To extract free polar metabolites, 10-30 mg of tissue was pulverized in liquid nitrogen using at Retsch Cryomill (#20.749.0001) and Retsch Cryomill Grinding Balls (#22.455.0002) for 2x 2min cycles at 25 Hz. Powdered tissue was extracted with 5:3:5 ice-cold methanol:water (with 13.3ng/µL Norvaline internal standard):chloroform. Extract was vortexted for 10min at 4˚C and centrifuged at for 10min at 20,000g at 4˚C in a benchtop centrifuge. An equal volume of the top (aqueous) phase was removed for each sample and evaporated under nitrogen and frozen at –80˚C for subsequent derivitization. Dried polar metabolites were dissolved in 1µL/mg tissue of 2% methoxyamine hydrochloride in pyridine (Thermo) and held at 37˚C for 1.5hr. After dissolution and reaction, tert–butyldimethylsilyl derivatization was initiated by adding 1.25µL/mg tissue *N*–methyl–*N*–(tert–butyldimethylsilyl)trifluoroacetamide + 1% tert–butyldimethylchlorosilane (Sigma) and incubating at 60˚C for 1hr.

The acid hydrolysis protocol was adapted from Antoniewicz and colleagues (*41*). Briefly, acid hydrolysis of tissue proteins was performed on snap frozen tissues by placing 1–5mg tissue in 1mL 18% hydrochloric acid overnight at 100˚C. 50µL supernatant was evaporated under nitrogen and frozen at –80˚C for subsequent derivitization. Dried hydrolysates were re–dissolved in pyridine (10µL/1mg tissue) prior to tert–butyldimethylsilyl derivatization, which was initiated by adding *N*–methyl–*N*–(tert–butyldimethylsilyl)trifluoroacetamide + 1% tert–butyldimethylchlorosilane (12.5µL/1mg tissue, Sigma) and incubating at 60˚C for 1h.

GC/MS analysis was performed using an Agilent 7890 GC equipped with a 30m DB–35MS capillary column connected to an Agilent 5975B MS operating under electron impact ionization

at 70eV. One microliter of sample was injected in splitless mode at 270°C, using helium as the carrier gas at a flow rate of 1mlmin^{-1}. For measurement of amino acids, the GC oven temperature was held at 100°C for 3min and increased to 300°C at 3.5°Cmin^{-1}. The MS source and quadrupole were held at 230°C and 150°C, respectively, and the detector was run in scanning mode, recording ion abundance in the range of 100–605 *m*/*z*. MIDs were determined by integrating the appropriate ion fragments (*41*) listed in table S7 and corrected for natural isotope abundance using an algorithm adapted from Ferandez and colleagues (*42*).

LC-MS Assessment of Stable Isotope Labeling

Tissue samples were collected and extracted as before. After drying the polar fraction, samples were resuspended in ice-cold 1:1 Acetonitrile:Water mix at 40µL/10mg tissue. LC/MS analyses were conducted on a QExactive benchtop orbitrap mass spectrometer equipped with a heated electrospray ionization (HESI) probe, which was coupled to a Dionex UltiMate 3000 UPLC system (Thermo Fisher Scientific, San Jose, CA). External mass calibration was performed using the standard calibration mixture every 7 days. For ^{13}C-BCAA tracing in tissues, 2.5 µl of each sample was injected into the LC/MS. For ^{15}N-BCAA tracing into nucleotides, 10 µl of each sample was injected into the LC/MS.

LC separation was performed on a ZIC-pHILIC 2.1 x 150 mm (5 µm particle size) column (EMD). Buffer A was 20 mM ammonium carbonate, 0.1% ammonium hydroxide; buffer B was acetonitrile. The chromatographic gradient was run at a flow rate of 0.150 ml/min as follows: 0-20 min.: linear gradient from 80% to 20% B; 20-20.5 min.: linear gradient from 20% to 80% B; 20.5-28 min.: hold at 80% B.

The mass spectrometer was operated with the spray voltage set to 3.0 kV, the heated capillary held at 275°C, and the HESI probe held at 350°C. The sheath gas flow was set to 40 units, the auxiliary gas flow was set to 15 units, and the sweep gas flow was set to 1 unit. For ^{13}C-BCAA tracing in tissues, the MS data acquisition was performed in full-scan, polarity switching mode in a range of 70-1000 m/z, with the resolution set at 70,000, the AGC target at 10^6, and the maximum injection time at 20 msec. For ^{15}N-BCAA tracing into nucleotides, the MS data were acquired in either positive or negative ion mode in a range of 285-385 m/z, with the resolution set at 140,000, the AGC target at 10^6, and the maximum injection time at 250 msec.

Relative quantitation of polar metabolites was performed with XCalibur QuanBrowser 2.2 (Thermo Fisher Scientific) using a 5 ppm mass tolerance and referencing an in-house library of chemical standards.

Tracer enrichment measurements were corrected for natural abundance for either ^{13}C or ^{15}N tracers as described by Yuan et al. (*43*).

Relative Abundance of Amino Acids in Tissue Samples

To determine the relative abundance of amino acids in the samples, protein hydrolysis with 18% hydrochloric acid was modified to include an amino acid internal standard mixture of U-^{13}C and U-^{15}N species (Cambridge Isotopes, # MSK-A2-1.2) at a final concentration of 100µM. The ratio of ion counts of unlabeled and fully labeled isotopomers of each amino acid was calculated. The fully labeled standards contain each amino acid at equal concentrations, so these calculated ratios represent their relative abundances. We therefore normalized the sum of these ratios to equal one to calculate the fraction of protein amino acids represented by each individual amino

acid. Cysteine and tryptophan residues are acid labile and not recoverable from the hydrolyzed samples.

DNA Isolation and Enzymatic DNA Digest

DNA was extracted using Phenol/Chloroform/Isoamyl extract mix (25:24:1 pH 8.0, Sigma P3803). DNA was precipitated with 0.1 volumes of 3M Sodium Acetate pH 5.2 and 3 volumes isopropanol overnight at -20°C. After pelleting and washing, DNA was resuspended in water. 20µL DNA was mixed with 6µL 100mM Succinic Acid-NaOH 50mM $CaCl_2$ pH5.9, 0.1µL 0.02U/µL Bovine Spleen Phosphodiesterase II (Sigma P9041), 0.1µL 2000GelUnits/µL Micrococcal Nuclease (NEB 0247) and incubated at 37°C for 2.5 hrs. Reaction was then extracted with 90µL 2:1 Chloroform:Methanol and the resulting methanol fraction was evaporated under nitrogen. Sample was resuspended in 50:50 Acetonitrile:Water at 100ng/µL for Q-Exactive Mass Spectroscopic Analysis.

RNA Extraction and qPCR

Approximately 10-20mg of frozen tissue was homogenized (ProScientific Pro200) in Trizol (Life Technologies) and RNA extracted according to the manufacturer's instructions. RNA concentration was determined using a Nanodrop (#ND1000) and 1µg of cDNA synthesized using iScript cDNA synthesis kit (BioRad). Quantitative-RT PCR was carried out on 5ng of cDNA using a final concentration of 2µM each of forward and reverse primers (table S8) with LuminoCt SYBR Green qPCR ReadyMix on a Roche Lightcycler II qPCR machine. Samples were normalized to the geometric mean of a panel of endogenous control genes (table S8) as previously described (*44*).

FACS Sorting and RNA isolation from Sorted Cells

Tumors were digested with 3mg/mL Dispase II (Roche), 1 mg/mL Collagenase I (Sigma), and 0.1mg/mL DNAse I (Sigma) in PBS for 30 mins at 37°C. To halt digestion, EDTA was then added to a final concentration of 10mM EDTA. Cells were strained through 70uM strainers and resuspended in flow cytometry staining buffer (eBioscience). Sytox Red (Life Technologies) was used for live/dead staining. Cell sorting was performed with a BD FACSAria III. RNA was isolated using the Ambion RNAqueous-Micro Total RNA Isolation Kit.

Protein Immunoblots

Approximately 20-30mg of frozen tissue was homogenized in RIPA buffer containing Protease Inhibitor Cocktail Tablets (Roche). Lysates were clarified by centrifugation in a benchtop centrifuge (Eppendorf Centrifugre 5145R) at 4˚C. Following clarification, protein concentration was determined using Bradford Protein Assay Dye (BioRad). All samples were run on SDS-acrylamide gels. After transfer to PVDF membrane and blocking in 5% BSA, blotting was performed using primary antibodies against Slc7a5 (Bioss, #bs-10125R), Bcat1 (Abcam, #ab110761), Bcat2 (Pierce Biotechnology, #PA5-21549), Bckdha (Novus Biologicals, #NBP1-79616), Hsp90 (Cell Signaling, #4877) and Vinculin (Sigma, # V9131). Secondary antibodies were goat anti-rabbit-HRP and goat-anti mouse (EMG Millipore). Western blot quantification was performing using ImageJ Image Analysis Software (NIH). Levels of BCAA catabolic enzymes were normalized to levels of vinculin and Hsp90.

Microarray expression data sets

Microarray expression data sets for pancreatic ductal adenocarcinoma, non-small cell lung cancer, and normal tissue were obtained from the NCBI GEO database (*30*) (accession numbers GSE15471, GSE16515, GSE71989 for pancreas samples and GSE18842 for lung samples) and were restricted to those using Affymetrix U133 Plus 2.0 GeneChips. The affyQCReport package from Bioconductor was used to search for poor quality chips. GeneChip arrays that passed quality control checks were normalized using the GCRMA (*45*) algorithm from Bioconductor. For each cancer type, tumor and normal samples from the same study were processed together.

The limma (*46*) method from Bioconductor was used to calculate differential expression of metabolic genes with results reported as ratios on the log2 scale. P-values for differential expression were corrected for multiple hypothesis testing using the Benjamini and Hochberg method (*47*), controlling for false discovery rate at 5%. Expression changes of all human genes assigned to metabolic pathways in the Kyoto Encyclopedia of Genes and Genomes (KEGG) (*48*) database were analyzed in addition to those assigned to the BCAA catabolic pathway.

TCGA RNA-seq data sets

Raw read counts were obtained from the Broad Firehose (https://gdac.broadinstitute.org/) LUAD and LUSQ January 28, 2016 data runs. Differential expression analysis was performed using the voom-limma (*48*) method from Bioconductor with results reported as ratios on the log2 scale. The Benjamini and Hochberg method was use to control the false discovery rate at 5%. Expression changes of metabolic genes in the KEGG database were analyzed in addition to those assigned to the BCAA catabolic pathway.

Principal Component Analysis and Hierarchical Cluster Analysis

Principal component analysis (PCA) was performed on qPCR expression data from mouse tumors and normal control tissues. The principal components were obtained by first mean-centering each variable and then scaling by the respective standard deviation. The correlation matrix was then calculated, along with the corresponding eigenvalues and eigenvectors.

Hierarchical cluster analysis was performed on log-transformed qPCR expression data from mouse tumors and normal control tissues. The complete linkage method and Euclidean distance metric were adopted for clustering.

Cell Lines

C57BL/6J KP NSCLC and PDAC ($KP^{-/-}C$) cell lines were derived as previously described (*18*). Briefly, end-stage tumors were dissected from indicated mice and mechanically chopped before trypsin disaggregation. Tumor cells were propagated in DMEM with 10% FBS, 4 mM glutamine and penicillin/streptomycin. Cell lines were tested and determined to be negative for mycoplasma.

Cell Culture

Isotope Tracing Experiments. For labeled-glutamine tracing, DMEM lacking glutamine was supplemented with [α-^{15}N]-glutamine (Cambridge Isotopes) to the standard DMEM concentration and with 10% dialyzed FBS. For leucine tracing, DMEM lacking leucine and containing either 4mM, 400μM or 40μM glutamine was supplemented with ^{15}N-leucine (Cambridge Isotopes) to the standard DMEM concentration and with 10% dialyzed FBS. For 3-

and 24-hr tracing experiment, $1x10^5$ cells were plated six hours prior to the start of the experiment.

Proliferation Assay. $1x10^4$ cells/well were plated and grown for four days in standard DMEM (without pyruvate) conditions with 10% FBS. Growth rate (in doublings/day) was calculated by the following equation:

$$\text{Doublings/day} = [\log_2(\#\text{cells day 4}/\#\text{cells day0})]/4\text{days}$$

Tracing Experiments for Bcat KO lines. DMEM media lacking leucine was supplemented with ^{15}N-leucine (Cambridge Isotopes) to the standard DMEM concentration and with 10% dialyzed FBS. For 24-hr tracing experiment, $1.5x10^5$ cells were plated six hours prior to the start of the experiment.

Slc7a5 Overexpression

The murine *Slc7a5* open reading frame was PCR amplified from a cDNA library obtained from Origene Technologies (Rockville, MD). The *Slc7a5* open reading frame was subcloned into pLHCX (Clontech, Mountain View, CA) by standard laboratory methods using the HindIII and ClaI restriction sites. The entire coding sequence of this construct was confirmed by sequencing analysis. Target PDAC cells were infected with either control empty vector or *Slc7a5*-expressing vector. Two *Slc7a5* cell lines (Lines A and B) were generated in parallel from different bacterial clones. Post-infection, cell lines were selected with hygromycin B for further experiments.

Leucine Uptake Assay

$1x10^5$ cells were plated the day before the experiment. At the start of the experiment, cells were washed once in PBS before exposure to PBS containing 200μM Leucine with 1μCi/mL [1-^{14}C]-leucine (American Radiolabeled Chemicals) for 0 min. or 2 min. at 37°C. Labeled media was aspirated and cells were washed 3x with excess ice-cold PBS before freezing in liquid nitrogen. Cells were extracted in 80% MetOH for measurement of radioactivity using scintillation counting.

Macropinocytosis Assay

Procedure. Macropinocytosis experiments were conducted as previously described (*49*) with the following modifications. Briefly, 2.5×10^4 NSCLC or PDAC cells were plated into 24-well plates containing fibronectin coated coverslips. Cells were cultured for 12 hours in 0.5mL DMEM containing 10% FBS, then media was removed and replaced with serum free DMEM for 24 hours. After serum starvation the media was replaced with serum free DMEM containing 10 ug/mL DQ Red BSA (Thermo-Fisher, D12051) and incubated for 30 minutes at 37°C. The media was then aspirated and the plate was washed 5 times with 2 mL ice cold PBS. Cells were fixed with 4% PFA for 15 minutes. Coverslips were removed and PDAC cells stained with 1ug/mL WGA 647 (Thermo-Fisher, W32466) for 15 minutes room temperature (NSCLC cells express GFP), and then both cell lines were stained with DAPI (Thermo-Fisher, D3571) for 10 minutes and mounted in Prolong Gold mounting media (Invitrogen P36934). Cells were then imaged on an applied precision DeltaVision Spectris Imaging System with a 60X objective. Macropinocytic index was calculated by field of view as described previously (*49*).

Analysis. Cell area was determined based on GFP fluorescence (NSCLC) or WGA-647 staining (PDAC) imaged in the FITC channel. DQ Red BSA was imaged in the Rhodamine

channel. Images were converted to 8-bit, Z-stacked, and thresholded using ImageJ. Cell area was read out using the "Measure" function, while DQ Red BSA area was calculated with the "Analyze Particles" function. The macropinocytic index was calculated by dividing the area of the particles by the cell area for each image.

CRISPR-Cas9 genome editing

SgRNA to *Bcat1* and *Bcat2* was designed by identifying exon sequence homology in *Bcat1* and *Bcat2* followed by an NGG PAM sequence (fig. S8A). An additional G was added to sgRNAs lacking a 5'G for U6 transcriptional initiation. U6-sgRNA-EFS-CAS9-2A-Puro vector was digested with BsmB1 and ligated with annealed sgRNAs. Lentivirus was produced by co-transfection of 293T cells with lentiviral backbone constructs and packaging vectors (delta8.2 and VSV-G) using TransIT-LT1 (Mirus Bio).

Implantation studies

Subcutaneous. For subcutaneous implantation studies, recipient mice were anesthetized with inhaled 2% isoflurane-oxygen mixture. 100μL of PBS containing 2.0 x 10^5 cells was delivered into the subcutaneous space on the hindflank of the animal. Volume estimates *in vivo* were calculated according to a modified ellipsoid volume equation:

$$\text{Tumor volume} = (4/3)\pi(\text{length}/2)(\text{width}/2)^2$$

Lung. For orthotopic implantation studies, recipient mice were anesthetized with inhaled 2% isoflurane-oxygen mixture. A catheter was inserted into the trachea and 50μL of PBS containing 2.0 x 10^5 cells delivered.

Pancreas. For orthotopic implantation studies, recipient mice were anesthetized with inhaled 2% isoflurane-oxygen mixture, a vertical incision made in the abdomen at the left mid-calvicular line, the spleen mobilized, and 50μL of either PBS or PBS containing 2.0 × 10^5 cells was injected into the tail of the pancreas. After sacrifice, tumors were dissected and calipered to get measurements of length, width and height. Tumor volume was then calculated for ellipsoid shaped tumors:

$$\text{Tumor volume} = (4/3)\pi(\text{length}/2)(\text{width}/2)(\text{height}/2)$$

Statistics

Appropriate statistical tests were performed where required. Two–sided unpaired student's *t*–tests were performed for all statistical analyses unless otherwise specified using Mircosoft Excel for Mac:2011 (Microsoft) or GraphPad Prism 6 (GraphPad Software). For example, two-way repeated measures *ANOVA* was used to assess for differences in subcutaneous allograft tumor growth over time and one-way *ANOVA* with Dunnett's multiple comparisons test used for tumor weight comparisons across three groups. No statistical method was used to pre-determine sample size.

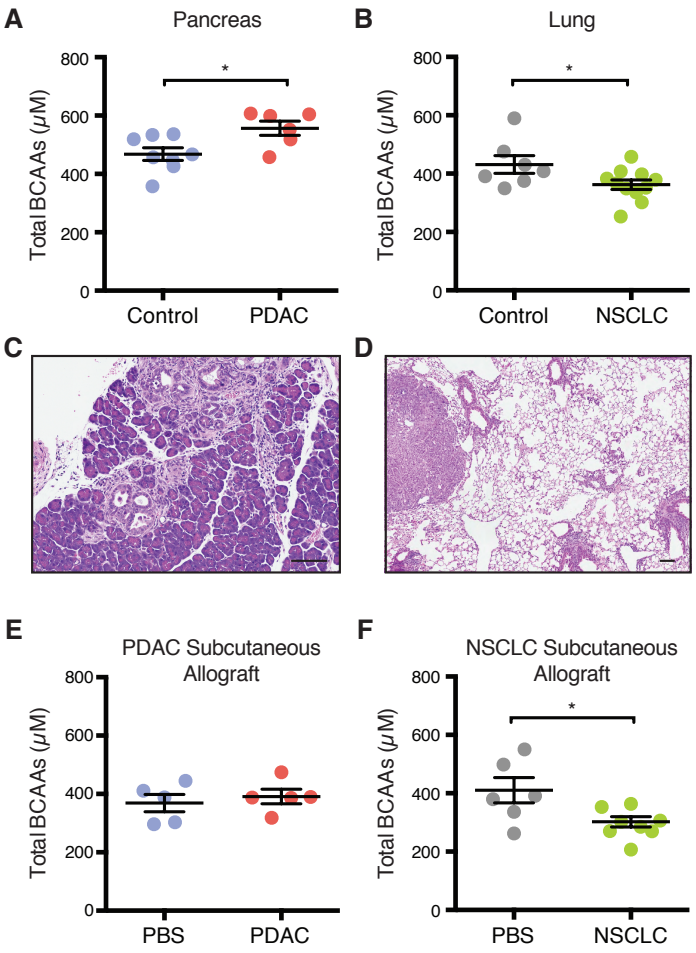

Fig. S1. Early pancreatic cancer and lung cancer have different effects on plasma BCAA levels.

(A) Plasma BCAA concentration in five-week-old control and PDAC mice. Data are presented as mean ± SEM. N = 8 control and N = 6 PDAC. (B) Plasma BCAA concentration eight weeks post-infection in control and NSCLC mice. Data are presented as mean ± SEM. N = 7 control and N = 11 NSCLC. (C) Representative H&E section from a five-week-old PDAC mouse showing areas of normal pancreas and tumor. Scale bar = 100μm. (D) Representative H&E section from an eight-weeks post-infection NSCLC mouse showing areas of normal lung and tumor. Scale bar = 100μm. (E) Plasma BCAA concentration in C57BL/6J mice four weeks after subcutaneous implantation of syngenic PDAC cells. Data are presented as mean ± SEM. N = 5 control, N = 5 PDAC. (F) Plasma BCAA concentration in C57BL/6J mice four weeks after subcutaneous implantation of syngenic NSCLC cells. Data are presented as mean ± SEM. N = 6 control, N = 7 NSCLC. Two-tailed t test was used for all comparisons between two groups. * P<0.05

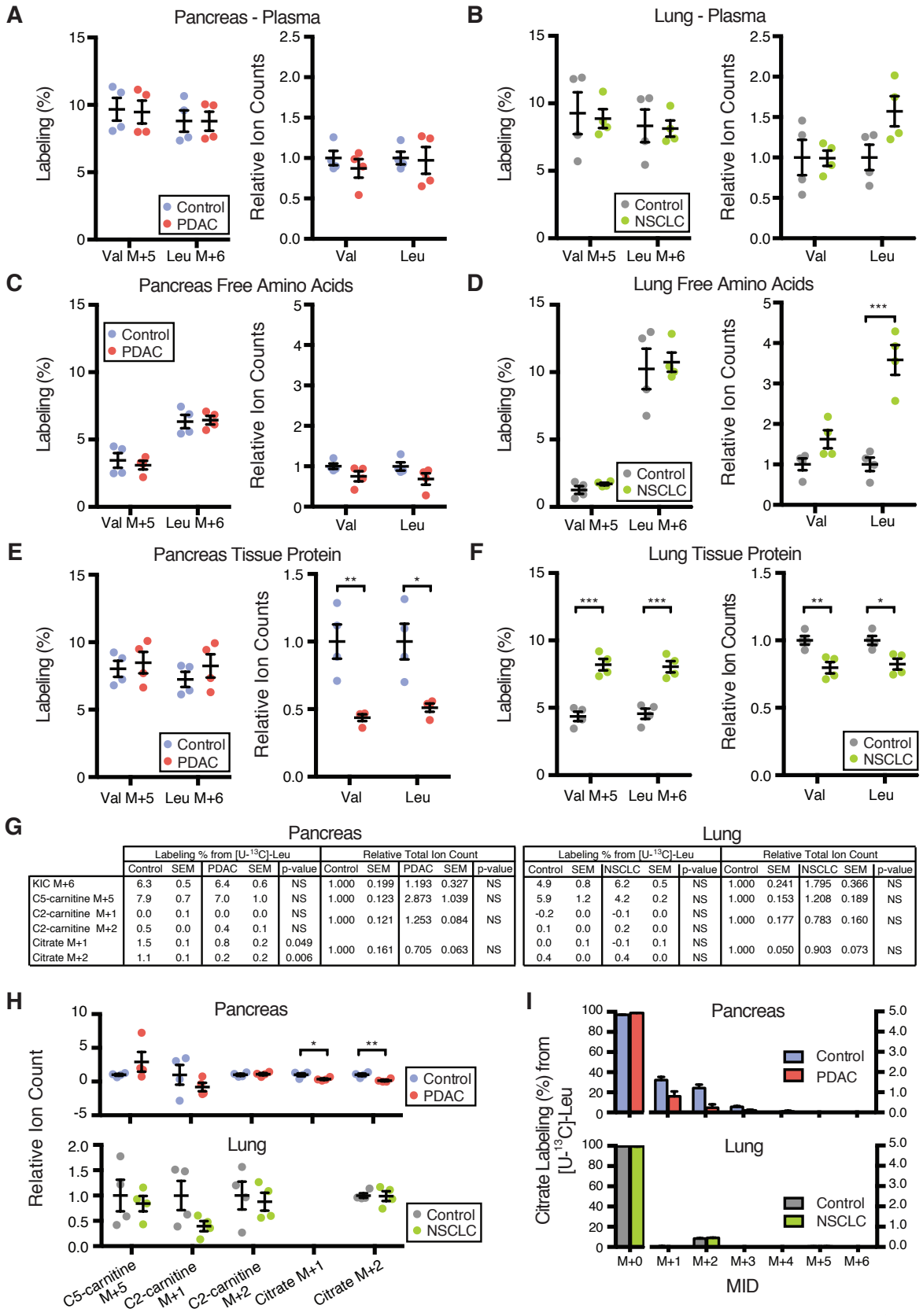

Pancreas	Labeling % from [U-^{13}C]-Leu					Relative Total Ion Count				
	Control	SEM	PDAC	SEM	p-value	Control	SEM	PDAC	SEM	p-value
KIC M+6	6.3	0.5	6.4	0.6	NS	1.000	0.199	1.193	0.327	NS
C5-carnitine M+5	7.9	0.7	7.0	1.0	NS	1.000	0.123	2.873	1.039	NS
C2-carnitine M+1	0.0	0.1	0.0	0.0	NS	1.000	0.121	1.253	0.084	NS
C2-carnitine M+2	0.5	0.0	0.4	0.1	NS					
Citrate M+1	1.5	0.1	0.8	0.2	0.049	1.000	0.161	0.705	0.063	NS
Citrate M+2	1.1	0.1	0.2	0.2	0.006					

Lung	Labeling % from [U-^{13}C]-Leu					Relative Total Ion Count				
	Control	SEM	NSCLC	SEM	p-value	Control	SEM	NSCLC	SEM	p-value
KIC M+6	4.9	0.8	6.2	0.5	NS	1.000	0.241	1.795	0.366	NS
C5-carnitine M+5	5.9	1.2	4.2	0.2	NS	1.000	0.153	1.208	0.189	NS
C2-carnitine M+1	-0.2	0.0	-0.1	0.0	NS	1.000	0.177	0.783	0.160	NS
C2-carnitine M+2	0.1	0.0	0.2	0.0	NS					
Citrate M+1	0.0	0.1	-0.1	0.1	NS	1.000	0.050	0.903	0.073	NS
Citrate M+2	0.4	0.0	0.4	0.0	NS					

Fig. S2. Mice with NSCLC display increased BCAA uptake and metabolism.

(A-I) Mice were fed ^{13}C-BCAA containing diet for seven days. (A) Percent plasma enrichment of fully labeled BCAAs (left panel) and relative ion counts of total BCAAs (right panel) in control and PDAC mice. Data are presented as mean ± SEM. $N = 4$ control and $N = 4$ PDAC. (B) Percent plasma enrichment of fully labeled BCAAs (left panel) and relative ion counts of total BCAAs (right panel) in control and NSCLC mice. Data are presented as mean ± SEM. $N = 4$ control and $N = 4$ NSCLC. (C) Percent enrichment of labeled free BCAAs (left panel) and relative ion counts of total free BCAAs (right panel) in control mouse pancreas tissues and PDAC mouse tumors. Data are presented as mean ± SEM. $N = 4$ control and $N = 4$ PDAC. (D) Percent enrichment of labeled free BCAAs (left panel) and relative ion counts of total free BCAAs (right panel) in control mouse lung tissues and NSCLC mouse tumors. Data are presented as mean ± SEM. $N = 4$ control and $N = 4$ NSCLC. (E) Percent enrichment of labeled BCAAs (left panel) and relative ion counts of total BCAAs (right panel) in protein hydrolysates of control mouse pancreas tissues and PDAC mouse tumors. Data are presented as mean ± SEM. $N = 4$ control and $N = 4$ PDAC. (F) Percent enrichment of labeled BCAAs (left panel) and relative ion counts of total BCAAs (right panel) in protein hydrolysates of control mouse lung tissues and NSCLC mouse tumors. Data are presented as mean ± SEM. $N = 4$ control and $N = 4$ NSCLC. (G) Labeling (%) from [U-^{13}C]-leucine and relative total ion count of downstream leucine metabolites (Fig. 1B) in tumors from PDAC and NSCLC mice and normal tissues from their respective control mice. Data are presented as mean ± SEM. $N = 4$ control and $N = 4$ PDAC; $N = 4$ control and $N = 4$ NSCLC. (H) Relative ion counts of labeled species downstream of KIC. Data are presented as mean ± SEM. Top panel, control mouse pancreas tissues and PDAC mouse tumors ($N = 4$ control and $N = 4$ PDAC) and bottom panel, control mouse lung tissues and NSCLC mouse tumors ($N = 4$ control and $N = 4$ NSCLC). (I) Citrate labeling (%) from [U-^{13}C]-leucine in PDAC and NSCLC. Data are presented as mean ± SEM. Top panel, $N = 4$ control and $N = 4$ PDAC. Bottom panel, $N = 4$ control and $N = 4$ NSCLC. MID = mass isotopomer distribution. Two-tailed *t* test was used for all comparisons between two groups. * $P<0.05$, ** $P<0.01$, *** $P<0.001$

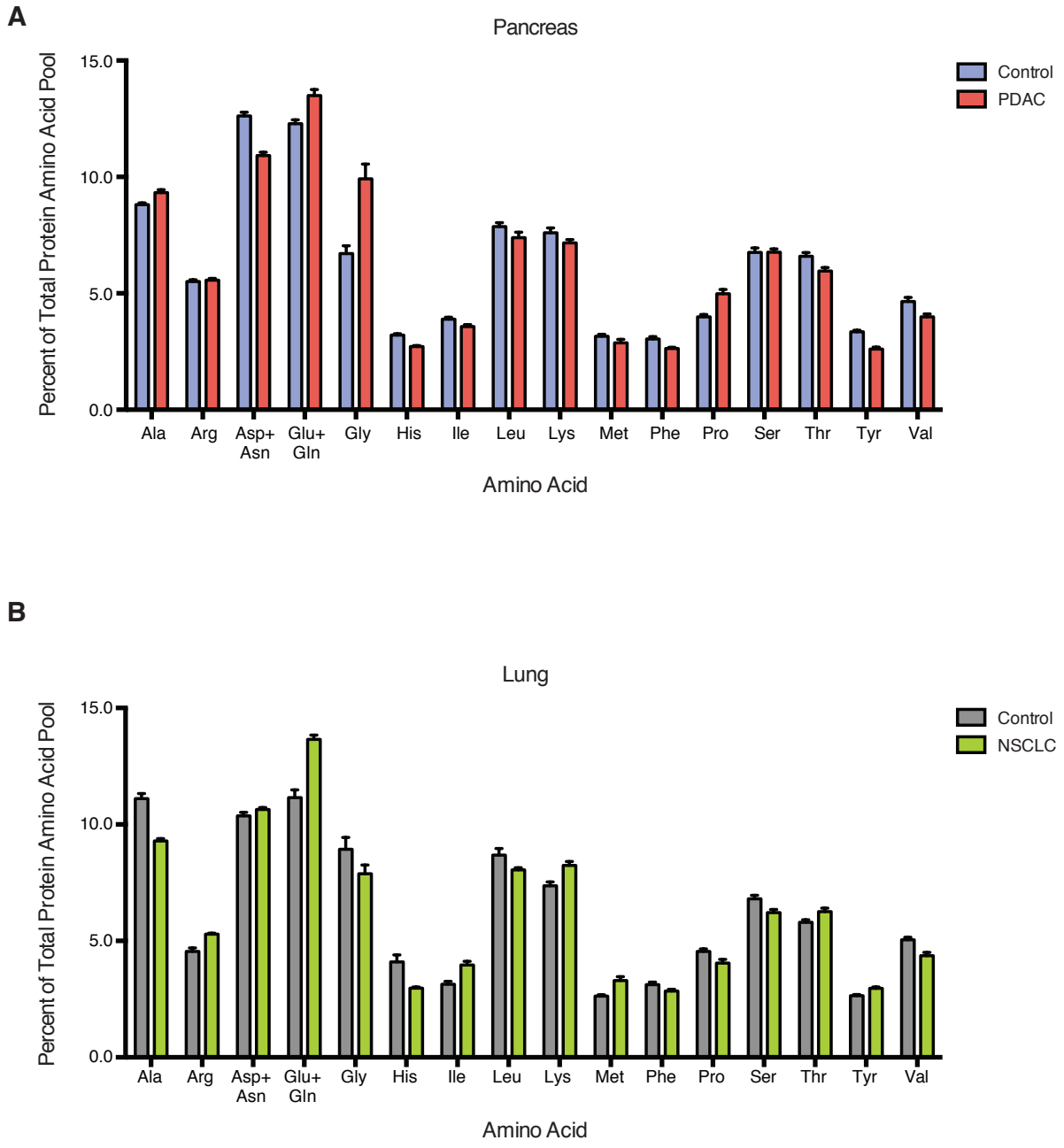

Fig. S3. Amino acid composition of PDAC and NSCLC tumors compared to control normal tissue.

(A) Percent of each amino acid in total tissue protein determined following acid hydrolysis of control pancreas and PDAC tumors. Data are presented as mean ± SEM. $N = 7$ control and $N = 5$ PDAC. (B) Percent of each amino acid in total tissue protein determined following acid hydrolysis of normal lung and NSCLC tumors. Data are presented as mean ± SEM. $N = 6$ control and $N = 6$ NSCLC.

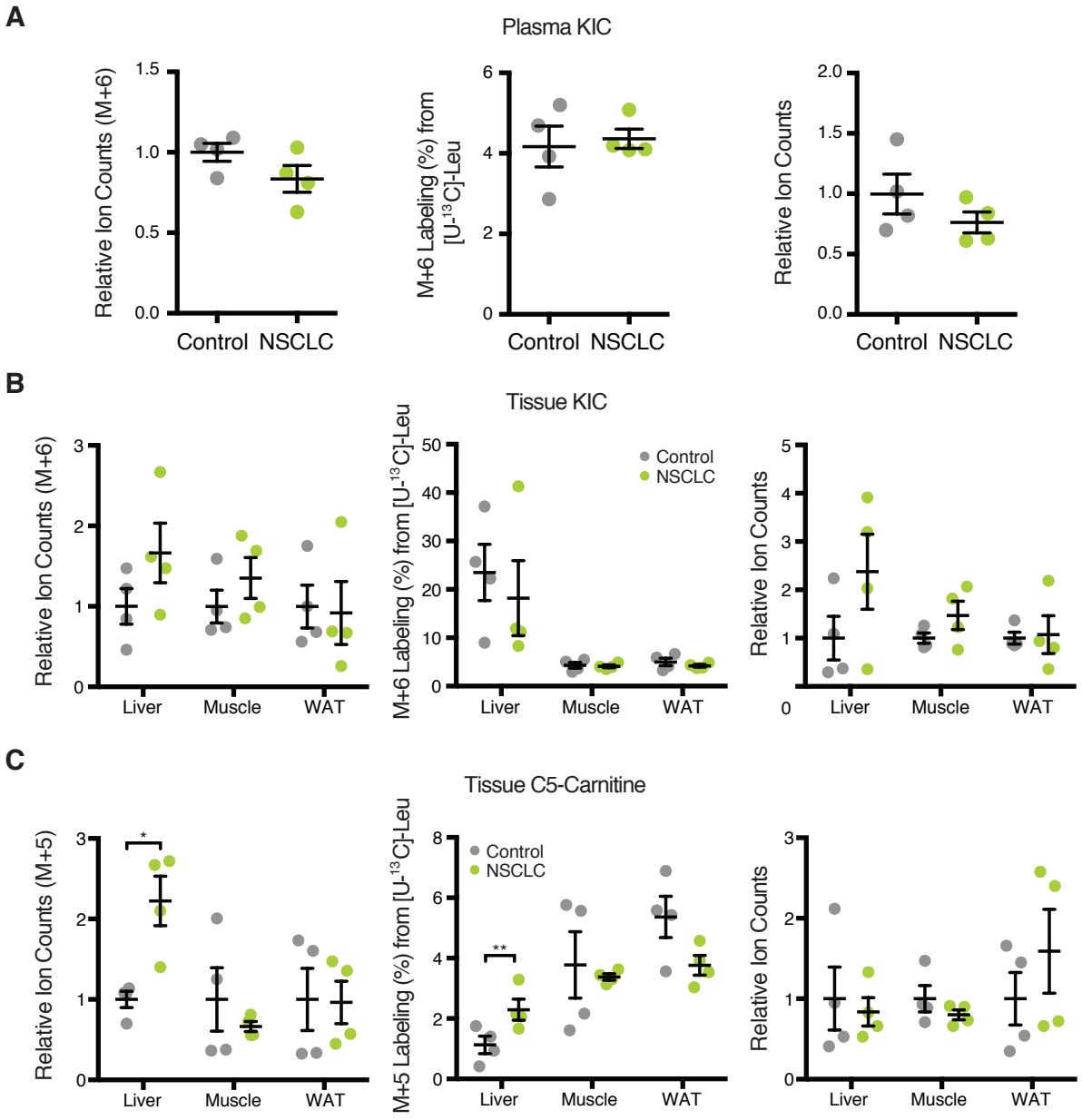
A
Plasma KIC
Relative Ion Counts (M+6)
1.5
1.0
0.5
0.0
Control NSCLC
M+6 Labeling (%) from [U-13C]-Leu
6
4
2
0
Control NSCLC
Relative Ion Counts
2.0
1.5
1.0
0.5
0.0
Control NSCLC
B
Tissue KIC
Relative Ion Counts (M+6)
3
2
1
0
Liver Muscle WAT
M+6 Labeling (%) from [U-13C]-Leu
50
40
30
20
10
0
Control
NSCLC
Liver Muscle WAT
Relative Ion Counts
5
4
3
2
1
0
Liver Muscle WAT
C
Tissue C5-Carnitine
Relative Ion Counts (M+5)
*
3
2
1
0
Liver Muscle WAT
M+5 Labeling (%) from [U-13C]-Leu
**
8
6
4
2
0
Control
NSCLC
Liver Muscle WAT
Relative Ion Counts
3
2
1
0
Liver Muscle WAT

Fig. S4. Evidence for liver oxidation of BCAA-derived carbon in NSCLC tumor-bearing mice.

(A-C) NSCLC mice were fed ^{13}C-BCAA containing diet for seven days. (A) Relative labeled ion counts of M+6 isotopomer (left), M+6 labeling (%) from [U-^{13}C]-leucine (center), and relative total ion counts (right) of KIC in the plasma of mice with NSCLC and their controls. Data are presented as mean ± SEM. $N = 4$ control and $N = 4$ NSCLC. (B) Relative labeled ion counts of M+6 isotopomer (left), M+6 labeling (%) from [U-^{13}C]-leucine (center), and relative total ion counts (right) of KIC in the liver, muscle (gastrocnemius) and perigonadal white adipose tissue (WAT) of mice with NSCLC and their controls. Data are presented as mean ± SEM. $N = 4$ control and $N = 4$ NSCLC. (C) Relative labeled ion counts of M+5 isotopomer (left), M+5 labeling (%) from [U-^{13}C]-leucine (center), and relative total ion counts (right) of C5-carnitine in the liver, muscle (gastrocnemius) and perigonadal white adipose tissue (WAT) of mice with NSCLC and their controls. Data are presented as mean ± SEM. $N = 4$ control and $N = 4$ NSCLC. Two-tailed *t* test was used for all comparisons between two groups. * $P<0.05$, ** $P<0.01$.

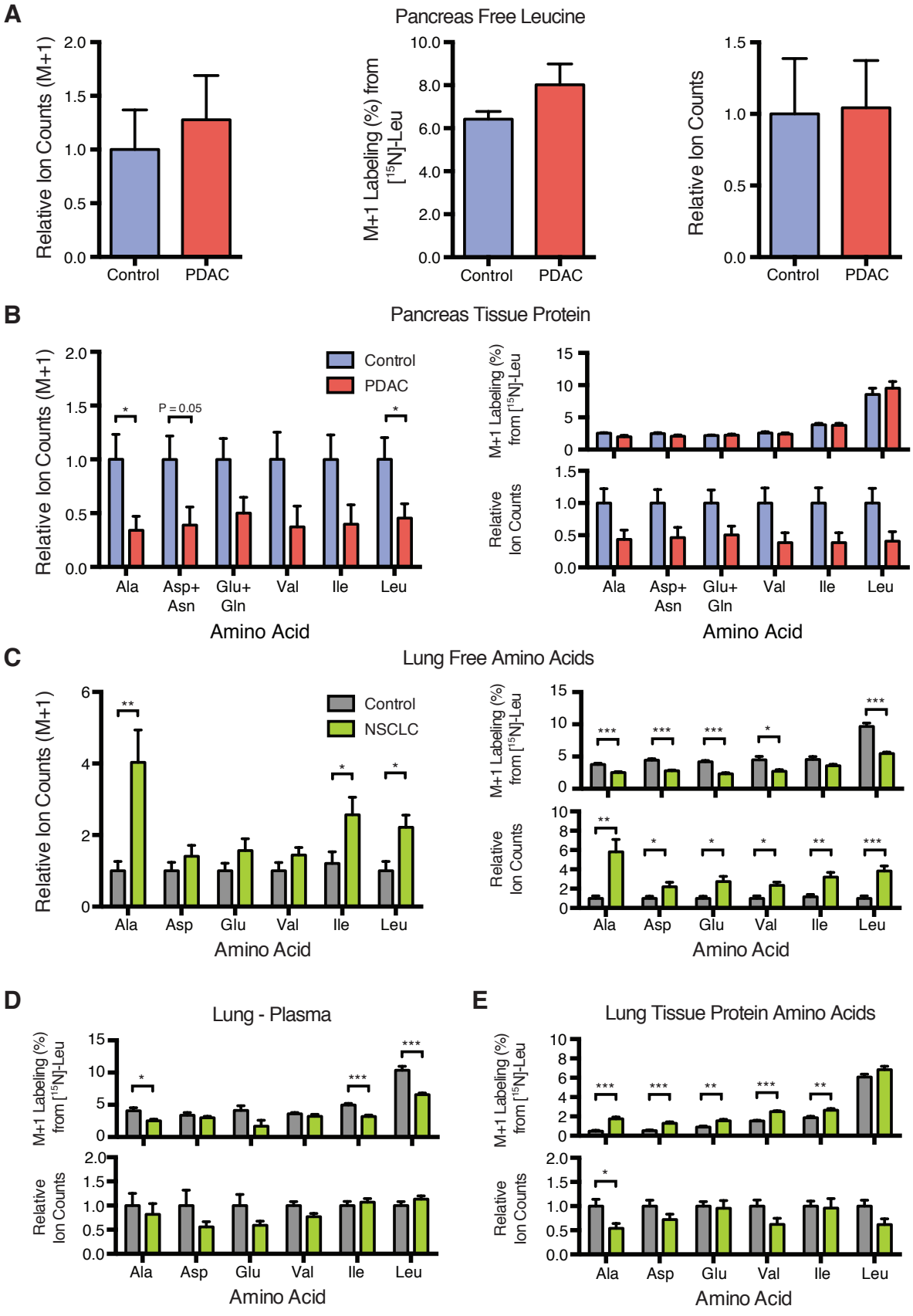
A
Pancreas Free Leucine
Relative Ion Counts (M+1)
M+1 Labeling (%) from [15N]-Leu
Relative Ion Counts
Control
PDAC
B
Pancreas Tissue Protein
Relative Ion Counts (M+1)
P = 0.05
M+1 Labeling (%) from [15N]-Leu
Relative Ion Counts
Ala
Asp+ Asn
Glu+ Gln
Val
Ile
Leu
Amino Acid
C
Lung Free Amino Acids
Control
NSCLC
Relative Ion Counts (M+1)
M+1 Labeling (%) from [15N]-Leu
Relative Ion Counts
Ala
Asp
Glu
Val
Ile
Leu
Amino Acid
D
Lung - Plasma
M+1 Labeling (%) from [15N]-Leu
Relative Ion Counts
Amino Acid
E
Lung Tissue Protein Amino Acids
M+1 Labeling (%) from [15N]-Leu
Relative Ion Counts
Amino Acid

Fig. S5. BCAA-derived nitrogen supports non-essential amino acid and DNA synthesis in NSCLC tumors.

(A-E) PDAC mice were fed ^{15}N-leucine containing diet for seven days and NSCLC mice were fed ^{15}N-leucine diet for six days. (A) Relative labeled ion counts of M+1 isotopomer (left), M+1 labeling (%) from ^{15}N-leucine (center), and relative total ion counts (right) of free leucine in control mouse pancreas tissues and PDAC mouse tumors. Data are presented as mean ± SEM. N = 6 control and N = 6 PDAC. (B) Relative labeled ion counts of M+1 isotopomers (left), M+1 labeing (%) from ^{15}N-leucine (top right), and relative total ion counts (bottom right) of amino acids from tissue protein hydrolysates in control mouse pancreas tissues and PDAC mouse tumors. Data are presented as mean ± SEM. N = 6 control and N = 6 PDAC. (C) Relative labeled ion counts of M+1 isotopomers (left), M+1 labeing (%) from ^{15}N-leucine (top right), and relative total ion counts (bottom right) of free amino acids in control mouse lung tissues and NSCLC mouse tumors. Data are presented as mean ± SEM. N = 6 control and N = 5 NSCLC. (D) M+1 labeing (%) from ^{15}N-leucine (top) and relative total ion counts (bottom) of free plasma amino acids in control and NSCLC mice. Data are presented as mean ± SEM. N = 5 control and N = 6 NSCLC. (E) M+1 labeing (%) from ^{15}N-leucine (top) and relative total ion counts (bottom) of free tissue amino acids in control mouse lung tissues and NSCLC mouse tumors. Data are presented as mean ± SEM. N = 6 control and N = 6 NSCLC. Two-tailed t test was used for all comparisons between two groups. * P<0.05, ** P<0.01, *** P<0.001

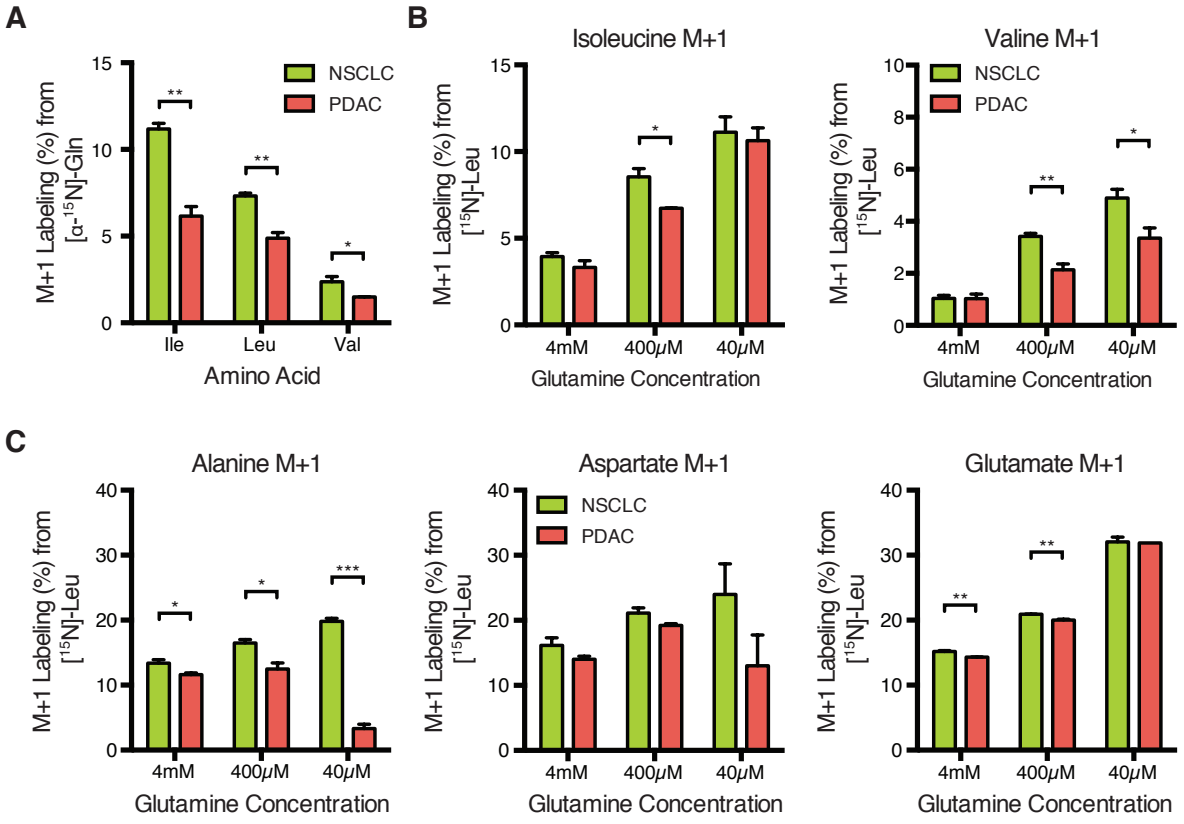

Fig. S6. Relationship between BCAA transamination and glutamine level *in vitro*.

(A) M+1 isoleucine (Ile), leucine (Leu) and valine (Val) labeling (%) from [α-^{15}N]-glutamine following exposure of PDAC or NSCLC cells for 24-hours to media containing [α-^{15}N]-glutamine. Data are presented as mean ± SEM. $N = 3$ per group. (B) M+1 isoleucine (left panel) and valine (right panel) labeling (%) from ^{15}N-leucine following exposure of PDAC or NSCLC cells for 3-hours to media containing ^{15}N-leucine and the indicated concentration of glutamine. Data are presented as mean ± SEM. $N = 3$ per group. (C) M+1 alanine (left panel), aspartate (middle panel) and glutamate (right panel) labeling (%) from ^{15}N-leucine following exposure of PDAC or NSCLC cells for 3-hours to media containing ^{15}N-leucine and the indicated concentration of glutamine. Data are presented as mean ± SEM. $N = 3$ per group. Two-tailed *t* test was used for all comparisons between two groups. * $P<0.05$, ** $P<0.01$, *** $P<0.001$

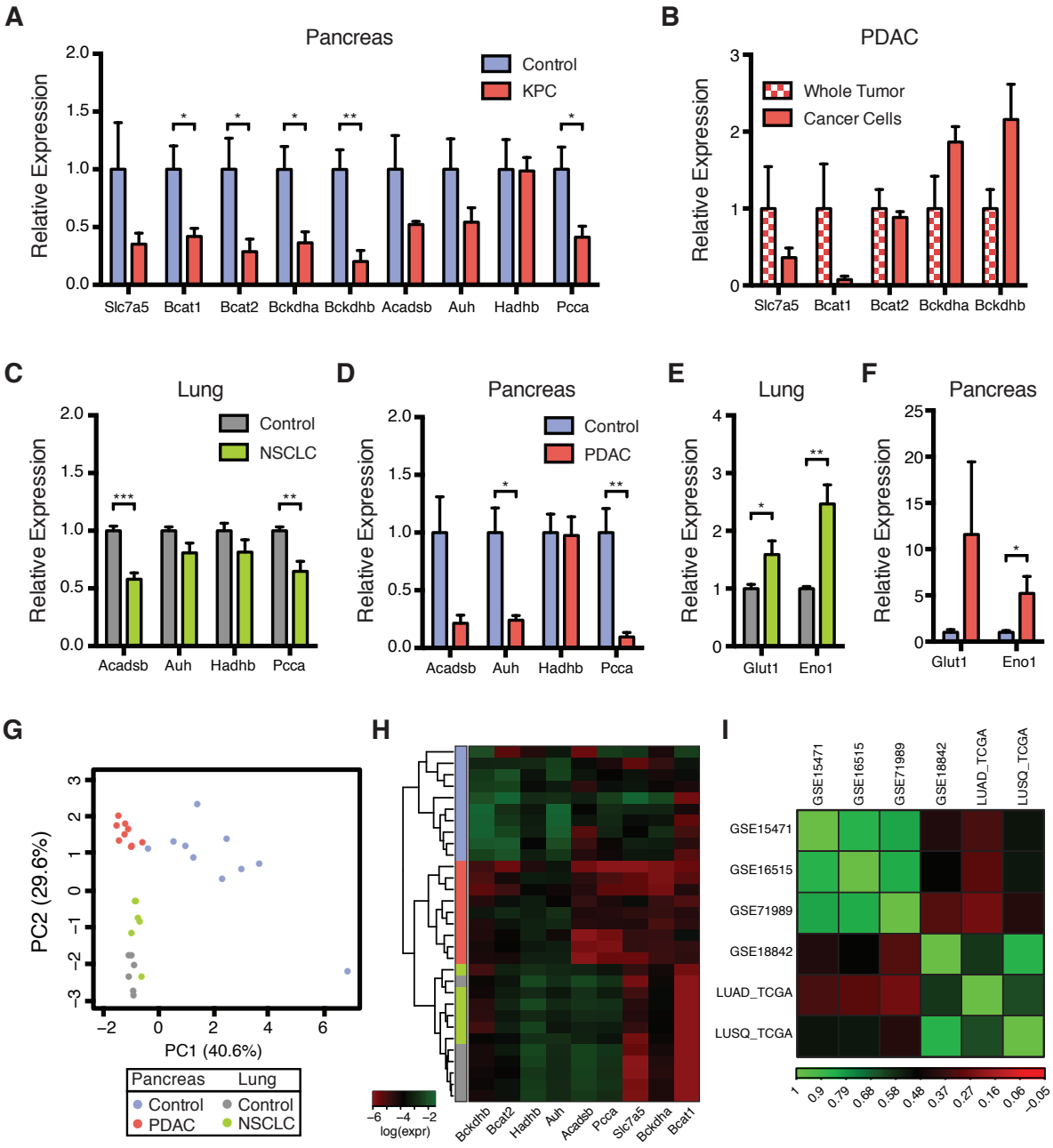
A
Pancreas
Control
KPC
Relative Expression
Slc7a5
Bcat1
Bcat2
Bckdha
Bckdhb
Acadsb
Auh
Hadhb
Pcca
B
PDAC
Whole Tumor
Cancer Cells
C
Lung
Control
NSCLC
D
Pancreas
Control
PDAC
E
Lung
Glut1
Eno1
F
Pancreas
G
PC2 (29.6%)
PC1 (40.6%)
Pancreas
Lung
Control
PDAC
Control
NSCLC
H
log(expr)
I
GSE15471
GSE16515
GSE71989
GSE18842
LUAD_TCGA
LUSQ_TCGA

Fig. S7. Gene expression in both mouse and human tumors reflects tumor tissue-specific BCAA metabolism.

(A) Relative expression of BCAA metabolic pathway genes in KPC PDAC tumors and normal pancreas. Data are presented as mean ± SEM. $N = 3$ control and $N = 4$ KPC. (B) Relative expression of BCAA metabolic pathway genes in FACS sorted tumor cells compared with parental whole tumor from $KP^{-/-}C$ PDAC mice. Data are presented as mean ± SEM. $N = 5$ tumors. Two-tailed paired-sample *t* test used for comparison. (C) Relative expression of downstream BCAA metabolic pathway genes in normal lung and NSCLC tumors from KP mice. Data are presented as mean ± SEM. $N = 6$ control and $N = 6$ NSCLC. (D) Relative expression of downstream BCAA metabolic pathway genes in normal pancreas and PDAC tumors from $KP^{-/-}C$ mice. Data are presented as mean ± SEM. $N = 7$ control and $N = 5$ PDAC. (E) Relative expression of glycolytic genes in normal lung and NSCLC tumors from KP mice. Data are presented as mean ± SEM. $N = 6$ control and $N = 6$ NSCLC. (F) Relative expression of glycolytic genes in normal pancreas and PDAC tumors from $KP^{-/-}C$ mice. Data are presented as mean ± SEM. $N = 7$ control and $N = 5$ PDAC. (G) Principal component analysis (PCA) of mouse BCAA catabolic gene expression in normal lung, NSCLC tumors, normal pancreas and PDAC tumors from Figs. 3, A and B and figs. S7, C and D. The first two principal components explained ~41% and ~30% of the variance respectively. (H) Hierarchical cluster analysis of mouse BCAA catabolic gene expression data. Colors on the side bar correspond to tissue samples given in fig. S7G. (I) Correlation of tumor expression fold-changes for branched-chain amino acid degradation pathway genes in human studies involving pancreas (GSE15471, GSE16515, GSE71989) and lung (GSE18842, LUAD_TCGA, LUSQ_TCGA). Average Spearman R was 0.84 for pancreas data. Spearman R with GSE18842 was 0.61 for lung adenocarcinoma and 0.86 for squamous cell carcinoma. Two-tailed *t* test was used for all comparisons unless otherwise stated. * $P<0.05$, ** $P<0.01$, *** $P<0.001$

A

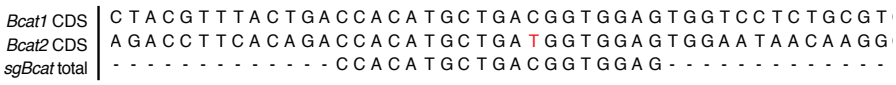

B

		Bcat1		*Bcat2*	
		Allele 1	Allele 2	Allele 1	Allele 2
NSCLC	Clone A	1bp insertion	8bp deletion	8bp deletion	5bp deletion
NSCLC	Clone B	1bp deletion	19bp deletion	25bp deletion	8bp deletion
PDAC		8bp deletion	8bp deletion	1bp deletion	2bp insertion

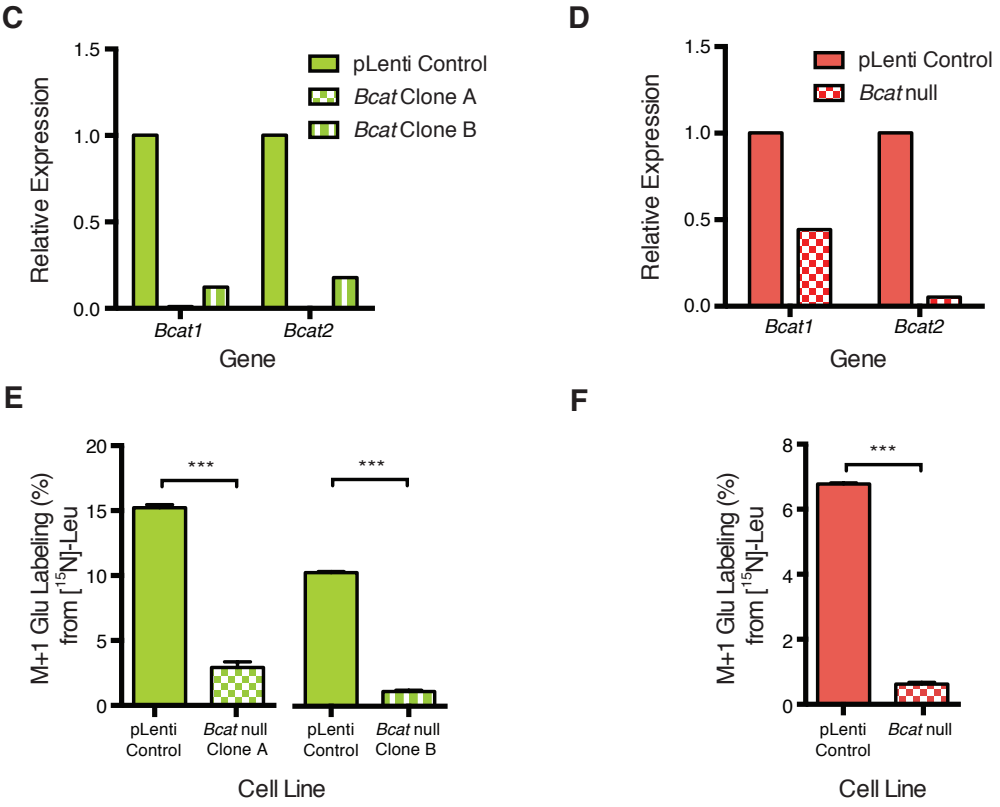

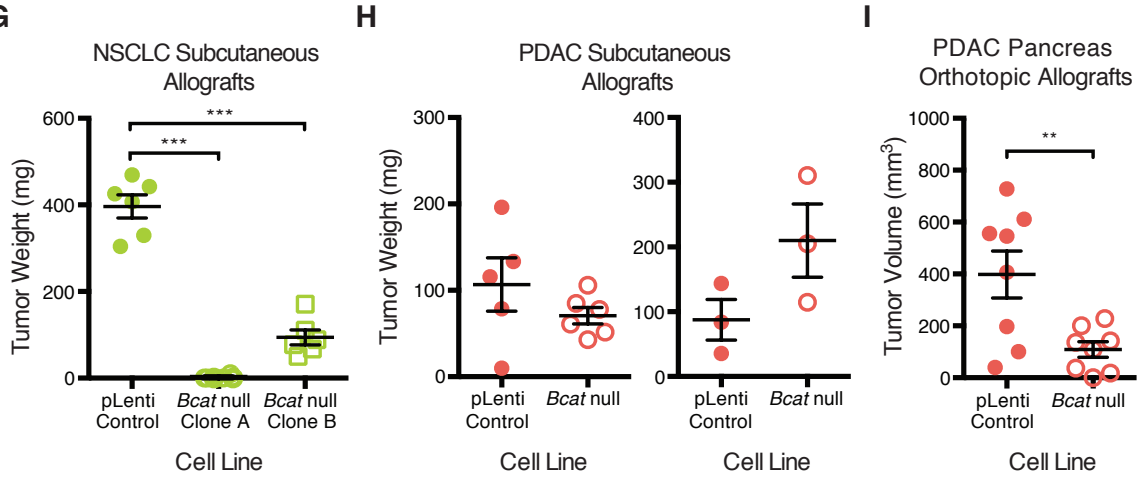

Fig. S8. Branched-chain amino acid transaminase (Bcat) activity is required for NSCLC tumor growth.

(A) Schematic of common exon sequence of *Bcat1* and *Bcat2* targeted with sgRNA for CRISPR-Cas9 genome editing. Red "T" highlights a 1bp sequence difference between the two isoforms. (B) Summary of sequence analyses of *Bcat1* and *Bcat2* in *Bcat* null clones derived from syngenic NSCLC and PDAC cell lines following sgRNA targeting with CRISPR-Cas9. (C) Normalized expression measured by qPCR of *Bcat1* and *Bcat2* in NSCLC *Bcat* null Clones A and B confirming decreased expression of both genes. (D) Normalized expression measured by qPCR of *Bcat1* and *Bcat2* in PDAC *Bcat* null cells confirming decreased expression of both genes. (E) M+1 Glu labeling (%) from ^{15}N-leucine following 24-hour ^{15}N-leucine tracing in control infected compared with NSCLC *Bcat* null Clone A and B cells. Data are presented as mean ± SEM. $N = 3$ per group. Representative experiment from ≥2 repeats. (F) M+1 Glu labeling (%) from ^{15}N-leucine following 24-hour ^{15}N-leucine tracing in control infected compared with PDAC *Bcat* null cells. Data are presented as mean ± SEM. $N = 3$ per group. (G) Tumor weight of subcutaneous allograft tumors generated from control infected and *Bcat* null syngenic NSCLC cell lines in C57BL/6J mice. Data are presented as mean ± SEM. $N = 6$ per group. (H) Two independent experiments determining tumor weight of subcutaneous allograft tumors derived from control infected and *Bcat* null syngenic PDAC cells in C57BL/6J mice. Data are presented as mean ± SEM. Left panel corresponds to mice in Fig. 4D. $N = 5$ pLenti control and $N = 6$ *Bcat* null. Right panel, $N = 3$ pLenti control and $N = 3$ *Bcat* null. (I) Calculated tumor volumes of orthotopically implanted syngenic PDAC pLenti control and *Bcat* null tumors. Data are presented as mean ± SEM. $N = 8$ per group. Two-tailed *t* test was used for all comparisons between two groups. * $P<0.05$, ** $P<0.01$, *** $P<0.001$

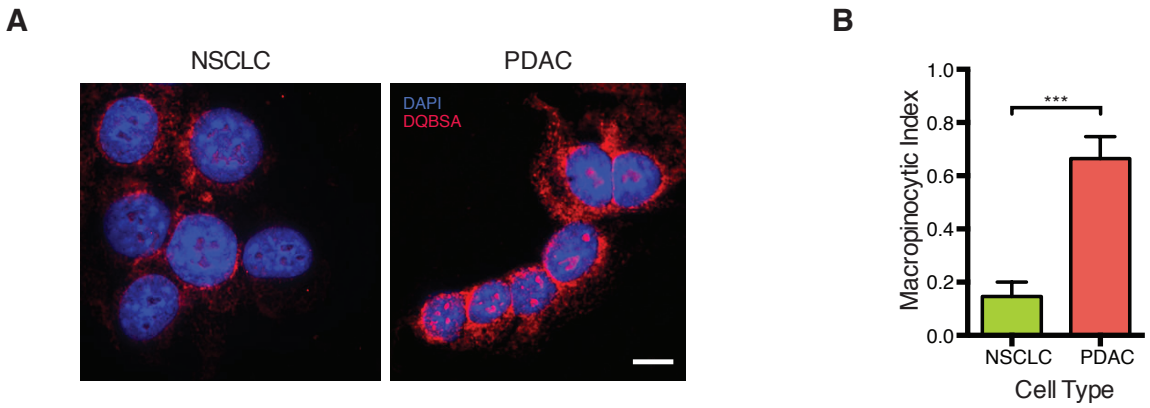

Fig. S9. NSCLC cells exhibit decreased macropinocytosis relative to PDAC cells.

(A) Representative images used to quantify macropinocytic uptake in NSCLC and PDAC cells. Cells were exposed to DQ Red BSA (DQBSA) and stained with DAPI. Scale bar = 10μm. (B) Quantified macropinocytic index based on fluorescence from DQBSA. Data were obtained from $N = 7$ fields-of-view (29 cells) for NSCLC and $N = 6$ fields-of-view (49 cells) for PDAC.

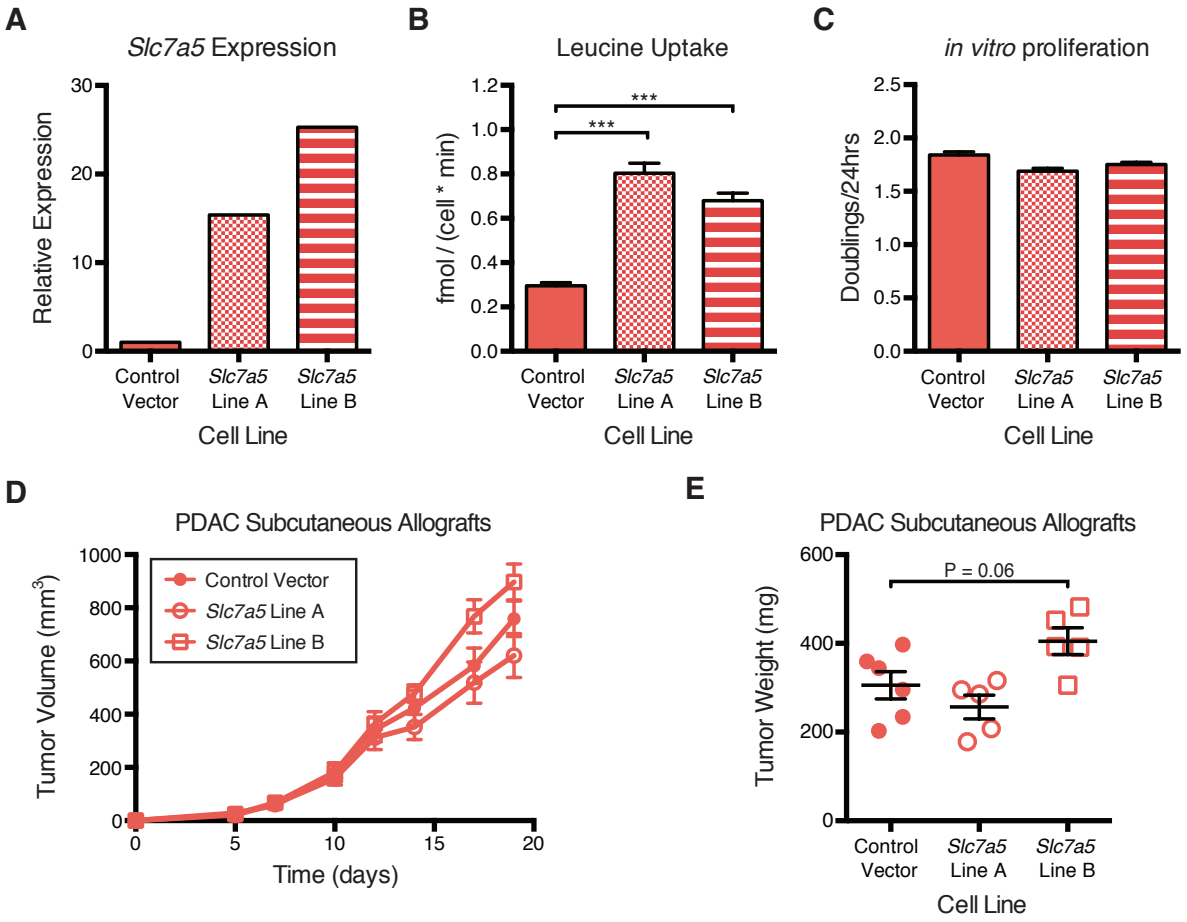

Fig. S10. Overexpression of *Slc7a5* in PDAC cells does not affect proliferation.

(A) Relative expression of *Slc7a5* in control infected PDAC cells and two PDAC cells lines overexpressing *Slc7a5*. (B) Uptake rate of leucine in vector control infected PDAC cells and PDAC cells overexpressing *Slc7a5*. Data are presented as mean ± SEM. $N = 3$ per group. One-way ordinary *ANOVA* with Dunnett's multiple comparisons for control vector versus each overexpression vector. (C) Doubling time *in vitro* of control infected and *Slc7a5* overexpressing PDAC cells. Data are presented as mean ± SEM. $N = 3$ per group. (D) Estimated tumor volume (mm^3) of subcutaneous allografts derived from control vector infected and *Slc7a5* overexpressing syngenic PDAC cell lines in C57BL/6J mice. Data are presented as mean ± SEM. $N = 6$ control vector and $N = 5$ each *Slc7a5* Vectors A and B. Two-way repeated measures *ANOVA* used for comparison between groups. (E) Tumor weight of subcutaneous allografts derived from control vector and *Slc7a5* overexpressing syngenic PDAC cells in C57BL/6J mice. Data are presented as mean ± SEM. $N = 6$ control vector and $N = 5$ each *Slc7a5* Vectors A and B. One-way ordinary *ANOVA* ($P = 0.0137$) with Dunnett's multiple comparisons for control vector versus each overexpression vector. * $P<0.05$, ** $P<0.01$, *** $P<0.001$

Table S1.

Human expression data comparing PDAC to adjacent normal pancreatic tissue (GSE15471).

Gene ID	Gene Symbol	Gene Name	log2 fold change	p-value
8140	SLC7A5	solute carrier family 7 (amino acid transporter light chain, L system), member 5	0.879502861	0.00122176
587	BCAT2	branched chain amino-acid transaminase 2, mitochondrial	-0.90281329	7.65E-05
586	BCAT1	branched chain amino-acid transaminase 1, cytosolic	-1.684103972	0.00477334
259307	IL4I1	interleukin 4 induced 1	0.232279522	0.034091294
593	BCKDHA	branched chain keto acid dehydrogenase E1, alpha polypeptide	-0.613720584	0.000701634
594	BCKDHB	branched chain keto acid dehydrogenase E1, beta polypeptide	-0.735076396	2.48E-06
1629	DBT	dihydrolipoamide branched chain transacylase E2	-0.587540291	0.000331659
1738	DLD	dihydrolipoamide dehydrogenase	-0.469580173	4.03E-08
35	ACADS	acyl-CoA dehydrogenase, C-2 to C-3 short chain	-0.877723342	1.46E-06
34	ACADM	acyl-CoA dehydrogenase, C-4 to C-12 straight chain	-0.928974891	9.48E-10
3712	IVD	isovaleryl-CoA dehydrogenase	-0.367787174	0.000388408
36	ACADSB	acyl-CoA dehydrogenase, short/branched chain	-1.373555807	4.44E-08
27034	ACAD8	acyl-CoA dehydrogenase family, member 8	-0.519219647	0.000294208
3030	HADHA	hydroxyacyl-CoA dehydrogenase/3-ketoacyl-CoA thiolase/enoyl-CoA hydratase (trifunctional protein), alpha subunit	-0.584595254	0.001003697
1962	EHHADH	enoyl-CoA, hydratase/3-hydroxyacyl CoA dehydrogenase	-0.658770531	0.003790345
1892	ECHS1	enoyl CoA hydratase, short chain, 1, mitochondrial	-0.048319001	0.745579334
3033	HADH	hydroxyacyl-CoA dehydrogenase	-0.547844188	0.001603
3028	HSD17B10	hydroxysteroid (17-beta) dehydrogenase 10	0.160472939	0.07307885
30	ACAA1	acetyl-CoA acyltransferase 1	-0.334432109	0.015971732
10449	ACAA2	acetyl-CoA acyltransferase 2	-0.566448642	4.78E-06
3032	HADHB	hydroxyacyl-CoA dehydrogenase/3-ketoacyl-CoA thiolase/enoyl-CoA hydratase (trifunctional protein), beta subunit	-0.246013864	0.009645609
5095	PCCA	propionyl CoA carboxylase, alpha polypeptide	-0.482286092	0.00036024
5096	PCCB	propionyl CoA carboxylase, beta polypeptide	-0.553229461	0.000186867
84693	MCEE	methylmalonyl CoA epimerase	-0.769948801	6.22E-05
4594	MUT	methylmalonyl CoA mutase	-0.454059405	7.59E-05
26275	HIBCH	3-hydroxyisobutyryl-CoA hydrolase	-0.725551273	2.74E-05
11112	HIBADH	3-hydroxyisobutyrate dehydrogenase	-0.346119019	0.005247236
4329	ALDH6A1	aldehyde dehydrogenase 6 family, member A1	-1.531300679	7.64E-09
217	ALDH2	aldehyde dehydrogenase 2 family (mitochondrial)	0.017059544	0.914989371
224	ALDH3A2	aldehyde dehydrogenase 3 family, member A2	-0.830408387	0.000415913
219	ALDH1B1	aldehyde dehydrogenase 1 family, member B1	-0.160216402	0.171935365
501	ALDH7A1	aldehyde dehydrogenase 7 family, member A1	-0.492505985	0.000172935
223	ALDH9A1	aldehyde dehydrogenase 9 family, member A1	-0.38849919	7.85E-06
316	AOX1	aldehyde oxidase 1	-1.714514255	0.001243926
18	ABAT	4-aminobutyrate aminotransferase	-1.913909607	3.47E-05
56922	MCCC1	methylcrotonoyl-CoA carboxylase 1 (alpha)	-0.807017307	2.65E-05
64087	MCCC2	methylcrotonoyl-CoA carboxylase 2 (beta)	-0.272774313	0.049069198

549	AUH	AU RNA binding protein/enoyl-CoA hydratase	-0.295488655	0.052464302
3155	HMGCL	3-hydroxymethyl-3-methylglutaryl-CoA lyase	-0.337595694	0.004458408
5019	OXCT1	3-oxoacid CoA transferase 1	0.537053005	0.003720935
64064	OXCT2	3-oxoacid CoA transferase 2	-0.533796167	4.00E-06
39	ACAT2	acetyl-CoA acetyltransferase 2	0.574014232	0.000803098
38	ACAT1	acetyl-CoA acetyltransferase 1	-1.309218369	5.31E-09
3157	HMGCS1	3-hydroxy-3-methylglutaryl-CoA synthase 1 (soluble)	0.08709899	0.513755372
3158	HMGCS2	3-hydroxy-3-methylglutaryl-CoA synthase 2 (mitochondrial)	-2.009941821	0.006996665

Table S2.

Human expression data comparing lung adenocarcinoma to adjacent normal lung tissue (GSE18842)

Gene ID	Gene Symbol	Gene Name	log2 fold change	p-value
8140	SLC7A5	solute carrier family 7 (amino acid transporter light chain, L system), member 5	2.526891751	6.23E-13
587	BCAT2	branched chain amino-acid transaminase 2, mitochondrial	0.453635541	0.003881953
586	BCAT1	branched chain amino-acid transaminase 1, cytosolic	0.807841298	0.013203348
259307	IL4I1	interleukin 4 induced 1	1.554637499	1.11E-06
593	BCKDHA	branched chain keto acid dehydrogenase E1, alpha polypeptide	0.226473838	0.073768274
594	BCKDHB	branched chain keto acid dehydrogenase E1, beta polypeptide	0.405589777	0.10000218
1629	DBT	dihydrolipoamide branched chain transacylase E2	0.711942322	0.000365403
1738	DLD	dihydrolipoamide dehydrogenase	0.322748437	0.005217065
35	ACADS	acyl-CoA dehydrogenase, C-2 to C-3 short chain	-0.372841503	0.000793325
34	ACADM	acyl-CoA dehydrogenase, C-4 to C-12 straight chain	-0.446473763	0.000226808
3712	IVD	isovaleryl-CoA dehydrogenase	-0.628354316	0.000721463
36	ACADSB	acyl-CoA dehydrogenase, short/branched chain	-1.695405701	2.78E-08
27034	ACAD8	acyl-CoA dehydrogenase family, member 8	-0.056757202	0.843774235
3030	HADHA	hydroxyacyl-CoA dehydrogenase/3-ketoacyl-CoA thiolase/enoyl-CoA hydratase (trifunctional protein), alpha subunit	-0.135673055	0.071471145
1962	EHHADH	enoyl-CoA, hydratase/3-hydroxyacyl CoA dehydrogenase	0.78441437	0.000216506
1892	ECHS1	enoyl CoA hydratase, short chain, 1, mitochondrial	0.485018276	2.15E-05
3033	HADH	hydroxyacyl-CoA dehydrogenase	0.219528794	0.207298092
3028	HSD17B10	hydroxysteroid (17-beta) dehydrogenase 10	0.670151503	4.40E-08
30	ACAA1	acetyl-CoA acyltransferase 1	-0.628902526	3.62E-07
10449	ACAA2	acetyl-CoA acyltransferase 2	-1.39255237	1.34E-07
3032	HADHB	hydroxyacyl-CoA dehydrogenase/3-ketoacyl-CoA thiolase/enoyl-CoA hydratase (trifunctional protein), beta subunit	-0.120032456	0.109495435
5095	PCCA	propionyl CoA carboxylase, alpha polypeptide	-0.428606571	0.013017158
5096	PCCB	propionyl CoA carboxylase, beta polypeptide	1.421420616	2.85E-11
84693	MCEE	methylmalonyl CoA epimerase	0.19575875	0.231716118
4594	MUT	methylmalonyl CoA mutase	-0.565339317	0.000718517
26275	HIBCH	3-hydroxyisobutyryl-CoA hydrolase	0.106494012	0.632709265
11112	HIBADH	3-hydroxyisobutyrate dehydrogenase	0.445133888	0.00299894
4329	ALDH6A1	aldehyde dehydrogenase 6 family, member A1	-0.656789044	0.001646638
217	ALDH2	aldehyde dehydrogenase 2 family (mitochondrial)	-1.742763109	1.15E-12
224	ALDH3A2	aldehyde dehydrogenase 3 family, member A2	-0.923729478	0.005218013
219	ALDH1B1	aldehyde dehydrogenase 1 family, member B1	0.960176481	5.93E-06
501	ALDH7A1	aldehyde dehydrogenase 7 family, member A1	-0.272075532	0.496164225
223	ALDH9A1	aldehyde dehydrogenase 9 family, member A1	-0.162836719	0.116324462
316	AOX1	aldehyde oxidase 1	-3.32817822	3.40E-20
18	ABAT	4-aminobutyrate aminotransferase	-0.64764613	0.125137447
56922	MCCC1	methylcrotonoyl-CoA carboxylase 1 (alpha)	0.388764727	0.051035278

64087	MCCC2	methylcrotonoyl-CoA carboxylase 2 (beta)	1.190292844	1.38E-09
549	AUH	AU RNA binding protein/enoyl-CoA hydratase	-0.3176852	0.044189772
3155	HMGCL	3-hydroxymethyl-3-methylglutaryl-CoA lyase	-0.097602498	0.570041016
5019	OXCT1	3-oxoacid CoA transferase 1	0.59930603	0.009009518
64064	OXCT2	3-oxoacid CoA transferase 2	-0.087938141	0.196592754
39	ACAT2	acetyl-CoA acetyltransferase 2	0.858717018	0.001369506
38	ACAT1	acetyl-CoA acetyltransferase 1	-0.823341597	3.09E-07
3157	HMGCS1	3-hydroxy-3-methylglutaryl-CoA synthase 1 (soluble)	1.414457463	0.000322578
3158	HMGCS2	3-hydroxy-3-methylglutaryl-CoA synthase 2 (mitochondrial)	-0.727162773	0.005448621

Table S3.

Human expression data comparing PDAC to adjacent normal pancreatic tissue (GSE16515).

Gene ID	Gene Symbol	Gene Name	log2 fold change	p-value
8140	SLC7A5	solute carrier family 7 (amino acid transporter light chain, L system), member 5	0.695729277	0.055891107
587	BCAT2	branched chain amino-acid transaminase 2, mitochondrial	-0.587343204	0.014782749
586	BCAT1	branched chain amino-acid transaminase 1, cytosolic	-0.89134623	0.097513629
259307	IL4I1	interleukin 4 induced 1	0.66088088	0.002497734
593	BCKDHA	branched chain keto acid dehydrogenase E1, alpha polypeptide	-0.396066507	0.097724294
594	BCKDHB	branched chain keto acid dehydrogenase E1, beta polypeptide	-0.29063685	0.075005553
1629	DBT	dihydrolipoamide branched chain transacylase E2	-0.55337088	0.010313609
1738	DLD	dihydrolipoamide dehydrogenase	-0.321787985	0.021112408
35	ACADS	acyl-CoA dehydrogenase, C-2 to C-3 short chain	-0.476142339	0.019639656
34	ACADM	acyl-CoA dehydrogenase, C-4 to C-12 straight chain	-0.823919118	3.92E-05
3712	IVD	isovaleryl-CoA dehydrogenase	0.109736254	0.497366466
36	ACADSB	acyl-CoA dehydrogenase, short/branched chain	-1.120427046	0.001225893
27034	ACAD8	acyl-CoA dehydrogenase family, member 8	-0.473503698	0.007574222
3030	HADHA	hydroxyacyl-CoA dehydrogenase/3-ketoacyl-CoA thiolase/enoyl-CoA hydratase (trifunctional protein), alpha subunit	-0.396494941	0.019975795
1962	EHHADH	enoyl-CoA, hydratase/3-hydroxyacyl CoA dehydrogenase	-0.245081107	0.374528225
1892	ECHS1	enoyl CoA hydratase, short chain, 1, mitochondrial	0.278663082	0.111478307
3033	HADH	hydroxyacyl-CoA dehydrogenase	-0.571526558	0.004666048
3028	HSD17B10	hydroxysteroid (17-beta) dehydrogenase 10	0.181845127	0.27170365
30	ACAA1	acetyl-CoA acyltransferase 1	0.092593182	0.690004538
10449	ACAA2	acetyl-CoA acyltransferase 2	-0.290889954	0.038773312
3032	HADHB	hydroxyacyl-CoA dehydrogenase/3-ketoacyl-CoA thiolase/enoyl-CoA hydratase (trifunctional protein), beta subunit	-0.152380334	0.298839704
5095	PCCA	propionyl CoA carboxylase, alpha polypeptide	-0.305848101	0.184914773
5096	PCCB	propionyl CoA carboxylase, beta polypeptide	-0.275083765	0.205200373
84693	MCEE	methylmalonyl CoA epimerase	-0.605450867	0.005927251
4594	MUT	methylmalonyl CoA mutase	-0.480169785	0.008284053
26275	HIBCH	3-hydroxyisobutyryl-CoA hydrolase	-0.230225489	0.292635698
11112	HIBADH	3-hydroxyisobutyrate dehydrogenase	0.193265533	0.361841563
4329	ALDH6A1	aldehyde dehydrogenase 6 family, member A1	-1.075354733	0.000108423
217	ALDH2	aldehyde dehydrogenase 2 family (mitochondrial)	0.191732118	0.389622882
224	ALDH3A2	aldehyde dehydrogenase 3 family, member A2	-0.638248983	0.014127821
219	ALDH1B1	aldehyde dehydrogenase 1 family, member B1	0.278048635	0.328069203
501	ALDH7A1	aldehyde dehydrogenase 7 family, member A1	-0.320432564	0.020145041
223	ALDH9A1	aldehyde dehydrogenase 9 family, member A1	-0.174329959	0.245888753
316	AOX1	aldehyde oxidase 1	-3.327431917	1.24E-05
18	ABAT	4-aminobutyrate aminotransferase	-1.997962017	0.000256669
56922	MCCC1	methylcrotonoyl-CoA carboxylase 1 (alpha)	-0.761894863	0.001967284
64087	MCCC2	methylcrotonoyl-CoA carboxylase 2 (beta)	0.369865204	0.069242708

549	AUH	AU RNA binding protein/enoyl-CoA hydratase	-0.426569359	0.012611638
3155	HMGCL	3-hydroxymethyl-3-methylglutaryl-CoA lyase	-0.253656494	0.086247239
5019	OXCT1	3-oxoacid CoA transferase 1	0.313890739	0.241161483
64064	OXCT2	3-oxoacid CoA transferase 2	-0.199144447	0.048316157
39	ACAT2	acetyl-CoA acetyltransferase 2	0.803807309	0.000849972
38	ACAT1	acetyl-CoA acetyltransferase 1	-1.556269919	8.38E-06
3157	HMGCS1	3-hydroxy-3-methylglutaryl-CoA synthase 1 (soluble)	1.430259689	0.004019182
3158	HMGCS2	3-hydroxy-3-methylglutaryl-CoA synthase 2 (mitochondrial)	-0.2944216	0.184121111

Table S4.

Human expression data comparing PDAC to adjacent normal pancreatic tissue (GSE71989).

Gene ID	Gene Symbol	Gene Name	log2 fold change	p-value
8140	SLC7A5	solute carrier family 7 (amino acid transporter light chain, L system), member 5	1.834506135	0.048832563
587	BCAT2	branched chain amino-acid transaminase 2, mitochondrial	-0.915125942	0.005263568
586	BCAT1	branched chain amino-acid transaminase 1, cytosolic	-3.353061454	0.000450364
259307	IL4I1	interleukin 4 induced 1	1.418006166	0.015636205
593	BCKDHA	branched chain keto acid dehydrogenase E1, alpha polypeptide	-1.148444992	0.001727003
594	BCKDHB	branched chain keto acid dehydrogenase E1, beta polypeptide	-0.687946873	0.156787101
1629	DBT	dihydrolipoamide branched chain transacylase E2	-2.138467417	4.04E-05
1738	DLD	dihydrolipoamide dehydrogenase	-0.309437161	0.194182069
35	ACADS	acyl-CoA dehydrogenase, C-2 to C-3 short chain	-0.781921247	0.001681216
34	ACADM	acyl-CoA dehydrogenase, C-4 to C-12 straight chain	-0.227530954	0.339717236
3712	IVD	isovaleryl-CoA dehydrogenase	0.364308007	0.136514652
36	ACADSB	acyl-CoA dehydrogenase, short/branched chain	-1.370334091	0.001696882
27034	ACAD8	acyl-CoA dehydrogenase family, member 8	-0.547440131	0.091116266
3030	HADHA	hydroxyacyl-CoA dehydrogenase/3-ketoacyl-CoA thiolase/enoyl-CoA hydratase (trifunctional protein), alpha subunit	-1.199004767	0.000134058
1962	EHHADH	enoyl-CoA, hydratase/3-hydroxyacyl CoA dehydrogenase	-0.456118174	0.175235142
1892	ECHS1	enoyl CoA hydratase, short chain, 1, mitochondrial	0.104757048	0.61074395
3033	HADH	hydroxyacyl-CoA dehydrogenase	-0.817026808	0.000522358
3028	HSD17B10	hydroxysteroid (17-beta) dehydrogenase 10	-0.218220037	0.082112071
30	ACAA1	acetyl-CoA acyltransferase 1	-0.243165988	0.078837838
10449	ACAA2	acetyl-CoA acyltransferase 2	-0.892178746	0.000406946
3032	HADHB	hydroxyacyl-CoA dehydrogenase/3-ketoacyl-CoA thiolase/enoyl-CoA hydratase (trifunctional protein), beta subunit	-0.176206766	0.336134576
5095	PCCA	propionyl CoA carboxylase, alpha polypeptide	-0.962865977	0.040167102
5096	PCCB	propionyl CoA carboxylase, beta polypeptide	-0.636381142	0.045189884
84693	MCEE	methylmalonyl CoA epimerase	-1.089729015	0.008120642
4594	MUT	methylmalonyl CoA mutase	-0.379457279	0.159824383
26275	HIBCH	3-hydroxyisobutyryl-CoA hydrolase	-0.604614912	0.049045949
11112	HIBADH	3-hydroxyisobutyrate dehydrogenase	-0.618580292	0.001237186
4329	ALDH6A1	aldehyde dehydrogenase 6 family, member A1	-1.980314485	0.006403709
217	ALDH2	aldehyde dehydrogenase 2 family (mitochondrial)	0.526938074	0.116496923
224	ALDH3A2	aldehyde dehydrogenase 3 family, member A2	-1.635199548	0.022669462
219	ALDH1B1	aldehyde dehydrogenase 1 family, member B1	-0.067959408	0.879445206
501	ALDH7A1	aldehyde dehydrogenase 7 family, member A1	-0.433351016	0.073731968
223	ALDH9A1	aldehyde dehydrogenase 9 family, member A1	-0.31800772	0.109525459
316	AOX1	aldehyde oxidase 1	-4.611602293	0.000559186
18	ABAT	4-aminobutyrate aminotransferase	-2.334970307	0.014544169
56922	MCCC1	methylcrotonoyl-CoA carboxylase 1 (alpha)	-1.16890529	0.001695464
64087	MCCC2	methylcrotonoyl-CoA carboxylase 2 (beta)	-0.275297083	0.213689093

549	AUH	AU RNA binding protein/enoyl-CoA hydratase	-0.595108622	0.036469128
3155	HMGCL	3-hydroxymethyl-3-methylglutaryl-CoA lyase	-0.160696682	0.441377191
5019	OXCT1	3-oxoacid CoA transferase 1	1.742802695	0.000484108
64064	OXCT2	3-oxoacid CoA transferase 2	-0.473291528	0.009046937
39	ACAT2	acetyl-CoA acetyltransferase 2	0.629875466	0.102936806
38	ACAT1	acetyl-CoA acetyltransferase 1	-1.624761864	0.001229512
3157	HMGCS1	3-hydroxy-3-methylglutaryl-CoA synthase 1 (soluble)	0.933801431	0.007789919
3158	HMGCS2	3-hydroxy-3-methylglutaryl-CoA synthase 2 (mitochondrial)	-0.404657124	0.008328684

Table S5.

Human expression data comparing lung adenocarcinoma to normal lung tissue (LUAD_TCGA)

Gene ID	Gene Symbol	logFC	AveExpr	t	P.Value	adj.P.Val	B
8140	SLC7A5	2.301489817	6.358231189	10.42262512	2.03E-23	1.99E-22	41.91341697
587	BCAT2	-0.022329943	5.405346113	-0.238943734	0.811234173	0.837543421	-7.962364892
586	BCAT1	-0.082200745	5.812571896	-0.390719929	0.696148682	0.734856037	-7.949366128
259307	IL4I1	1.802053865	3.662717891	7.146453383	2.70E-12	1.13E-11	16.96043713
593	BCKDHA	-0.064986379	5.742374666	-0.805448303	0.420893276	0.471526877	-7.695807869
594	BCKDHB	-0.089449287	3.848210819	-1.05811492	0.290446434	0.338490079	-7.215969219
1629	DBT	-0.165486395	4.901371519	-2.308007721	0.021351989	0.030447339	-5.296980892
1738	DLD	0.037319195	6.153408635	0.518807164	0.604094408	0.648584069	-7.903129538
35	ACADS	-0.396142929	4.654196909	-3.721228554	0.000217685	0.000404804	-1.096055568
34	ACADM	-0.149175994	5.561180575	-1.893454362	0.058798186	0.078016723	-6.224218221
3712	IVD	-0.454413704	6.120665928	-4.234544074	2.67E-05	5.56E-05	0.78537962
36	ACADSB	-0.656685952	5.224157391	-5.221457536	2.48E-07	6.60E-07	5.310708694
27034	ACAD8	0.952248253	5.346434799	6.865131266	1.72E-11	6.71E-11	14.77617986
3030	HADHA	-0.16085849	7.678322593	-3.398825913	0.000723518	0.001259949	-2.325968325
1962	EHHADH	0.029588819	3.912137766	0.267564907	0.789129991	0.818635495	-7.734194387
1892	ECHS1	0.496639082	6.83135147	6.780040815	2.98E-11	1.13E-10	14.08150294
3033	HADH	-0.073366638	5.661570217	-0.888721427	0.374523663	0.425039729	-7.619794388
3028	HSD17B10	0.506258189	5.855151605	6.499293438	1.75E-10	6.21E-10	12.40300803
30	ACAA1	-0.407743414	5.772675264	-5.017906592	6.97E-07	1.77E-06	4.293828537
10449	ACAA2	-0.837258146	5.703806931	-8.277737019	8.78E-16	4.84E-15	24.34694946
3032	HADHB	-0.021523161	6.805987063	-0.408996065	0.682694521	0.722433188	-7.971203158
5095	PCCA	-0.246456074	3.753144879	-2.016385373	0.044223175	0.059868769	-5.753673006
5096	PCCB	0.343767432	5.710113172	4.699194071	3.27E-06	7.66E-06	2.850605682
84693	MCEE	0.132703208	2.801890502	1.308484783	0.191230609	0.232045672	-6.694952278
4594	MUT	0.11151478	5.342882293	1.519870588	0.129092016	0.161790721	-6.820741756
26275	HIBCH	0.207361423	4.500464409	2.463148936	0.014063513	0.020557426	-4.826842489
11112	HIBADH	0.546603418	5.672095469	6.273912746	6.92E-10	2.33E-09	11.07907501
4329	ALDH6A1	-0.143182697	3.97983577	-1.19603012	0.232176743	0.276353846	-7.092230071
217	ALDH2	-1.376449884	8.081884479	-10.37850121	2.99E-23	2.89E-22	41.38215198
224	ALDH3A2	-0.455354534	7.29385346	-3.207001887	0.001415631	0.002381613	-2.950344994
219	ALDH1B1	0.947103168	5.207573479	7.848908012	2.05E-14	1.02E-13	21.41181195
501	ALDH7A1	0.165878163	5.557560458	1.785293215	0.074739652	0.097505234	-6.400096771
223	ALDH9A1	-0.23186742	6.512121218	-3.239786141	0.00126511	0.002143239	-2.849056789
316	AOX1	-2.15049672	2.471108098	-12.67670724	1.18E-32	2.09E-31	63.05942585
18	ABAT	-0.270201151	3.825653793	-1.616717801	0.106486521	0.135456773	-6.492303448
56922	MCCC1	-0.310875957	5.036842343	-3.089395627	0.002102324	0.003454369	-3.242611828
64087	MCCC2	0.60856239	6.249504932	7.598211993	1.22E-13	5.69E-13	19.51128747
549	AUH	-0.307891419	3.26732002	-4.000960494	7.13E-05	0.000141411	0.193214559

3155	HMGCL	0.094091401	5.573266149	1.277615691	0.20189947	0.243699726	-7.181453788
5019	OXCT1	0.035856218	4.423932006	0.217854779	0.827619389	0.851982284	-7.835471736
64064	OXCT2	0.753014278	-1.341418463	3.932433184	9.43E-05	0.00018367	0.41322003
39	ACAT2	-0.435561364	4.614165503	-4.402822034	1.27E-05	2.77E-05	1.596491751
38	ACAT1	-0.637666221	5.665301524	-6.551388268	1.27E-10	4.55E-10	12.67279193
3157	HMGCS1	-1.093236292	6.104568228	-9.63348088	1.82E-20	1.43E-19	34.99752964
3158	HMGCS2	-3.494020182	-1.784574072	-8.586127586	8.40E-17	5.02E-16	27.27033633

Table S6.

Human expression data comparing lung squamous cell carcinoma to normal lung tissue (LUSQ_TCGA)

Gene ID	Gene Symbol	logFC	AveExpr	t	P.Value	adj.P.Val	B
8140	SLC7A5	3.43564825	7.707835006	16.8420549	1.06E-51	1.70E-50	106.4644738
587	BCAT2	0.07009414	5.318307538	0.789526849	0.430141792	0.462844102	-7.897165607
586	BCAT1	-0.688161797	5.359877887	-3.719734352	0.000219746	0.000334717	-1.397369172
259307	IL4I1	1.296770374	3.453601085	6.269297405	7.30E-10	1.73E-09	11.21977782
593	BCKDHA	0.079824619	5.779109943	0.928442663	0.353582178	0.386300753	-7.802215369
594	BCKDHB	-0.07226825	3.684809521	-0.840701212	0.400877901	0.433848221	-7.671861771
1629	DBT	0.164670241	5.022387251	2.257039152	0.024394191	0.030722493	-5.64125545
1738	DLD	0.472083711	6.473703967	5.931205524	5.30E-09	1.19E-08	8.827576396
35	ACADS	-0.688906151	4.141312537	-8.68132614	4.38E-17	1.54E-16	27.21097897
34	ACADM	-0.371239168	5.144530653	-4.691191107	3.43E-06	6.16E-06	2.582944004
3712	IVD	-0.645242161	5.791703655	-6.78309739	3.03E-11	7.80E-11	13.8768321
36	ACADSB	-0.937195974	4.796808291	-8.847962164	1.19E-17	4.34E-17	28.43082989
27034	ACAD8	-0.2502558	4.257898037	-3.025178338	0.002600091	0.003600605	-3.58739773
3030	HADHA	-0.048020113	7.710428249	-0.821136923	0.411921353	0.444919058	-7.911004339
1962	EHHADH	1.034244319	4.674421838	8.219699856	1.45E-15	4.76E-15	23.86230287
1892	ECHS1	0.451173254	6.698471514	5.523701135	5.11E-08	1.08E-07	6.617537985
3033	HADH	0.009166245	5.628533204	0.10419606	0.917051457	0.925609627	-8.224064291
3028	HSD17B10	0.868935793	6.207759135	10.67223442	2.61E-24	1.33E-23	43.62216891
30	ACAA1	-0.833287959	5.297952201	-12.55693223	5.29E-32	3.90E-31	61.21244863
10449	ACAA2	-1.598338832	4.859858995	-11.46266038	1.91E-27	1.13E-26	50.77961214
3032	HADHB	0.085773364	6.782436419	1.478288742	0.1398986	0.16181226	-7.160907287
5095	PCCA	-0.633654611	3.330750953	-7.456879784	3.44E-13	9.94E-13	18.47590952
5096	PCCB	0.842988114	6.090580657	9.092035539	1.72E-18	6.55E-18	30.34813146
84693	MCEE	-0.141246973	2.454128328	-1.802403963	0.072025057	0.086354068	-6.183095022
4594	MUT	0.09017852	5.215313953	1.228996733	0.219594598	0.247453796	-7.445942964
26275	HIBCH	0.259467139	4.413522371	2.712491386	0.006885437	0.009149068	-4.440336234
11112	HIBADH	0.331576682	5.35150903	4.126505311	4.25E-05	6.89E-05	0.198328863
4329	ALDH6A1	-0.883081122	3.325422375	-9.281187504	3.75E-19	1.48E-18	31.99751141
217	ALDH2	-2.311539127	7.018829786	-17.05700482	9.50E-53	1.60E-51	108.8074819
224	ALDH3A2	-0.459840083	7.056178264	-3.137152311	0.001796571	0.002524887	-3.367434368
219	ALDH1B1	0.740029643	5.111153608	6.320069534	5.38E-10	1.29E-09	11.16559328
501	ALDH7A1	-0.906626359	4.440622329	-4.201445115	3.09E-05	5.08E-05	0.499215659
223	ALDH9A1	-0.10132745	6.470811855	-1.225070269	0.221069152	0.249042786	-7.501370219
316	AOX1	-3.443645528	1.534859041	-23.28947731	3.58E-84	1.74E-82	181.1221231
18	ABAT	-0.815746782	3.178580439	-5.589189087	3.58E-08	7.66E-08	7.171077491
56922	MCCC1	0.554866022	5.692969451	4.016982659	6.71E-05	0.000107042	-0.247020887
64087	MCCC2	0.456443463	6.070667953	5.888844777	6.75E-09	1.51E-08	8.60376602

549	AUH	-0.377647125	3.065586136	-5.361194814	1.22E-07	2.51E-07	6.064739271
3155	HMGCL	-0.344838377	5.090438162	-4.626389578	4.64E-06	8.23E-06	2.296688655
5019	OXCT1	0.916244765	5.228583589	6.940823736	1.09E-11	2.90E-11	14.98423096
64064	OXCT2	0.136104799	-1.86673463	0.658902471	0.510232056	0.543357378	-7.109385516
39	ACAT2	0.588374543	5.528288775	4.66015788	3.96E-06	7.08E-06	2.469036769
38	ACAT1	-0.93819422	5.172873981	-11.63615179	3.76E-28	2.31E-27	52.39608243
3157	HMGCS1	0.255430691	7.291842146	1.752511445	0.080238867	0.095618141	-6.719621068
3158	HMGCS2	-4.265592639	-3.501736693	-10.30012009	6.98E-23	3.32E-22	40.98001202

Table S7.

Metabolite Fragments Used for Isotope Quantification in GC/MS analysis

Metabolite	Carbons	Formula	m/z
Leu	123456	$C_{14}H_{32}O_2NSi_2$	302
Ile	123456	$C_{14}H_{32}O_2NSi_2$	302
Val	12345	$C_{13}H_{30}O_2NSi_2$	288
Ala	123	$C_{11}H_{26}O_2NSi_2$	260
Asp	1234	$C_{18}H_{40}O_3NSi_3$	418
Glu	12345	$C_{19}H_{42}O_4NSi_3$	432
Lys	123456	$C_{20}H_{47}O_2N_2Si_3$	431
Citrate	123456	$C_{26}H_{55}O_7Si_4$	591

Table S8.

qRT-PCR Primer Sets

Gene	Forward (5' → 3')	Reverse (5' → 3')
Slc7a5	ATATCACGCTGCTCAACGGTG	CTCCAGCATGTAGGCGTAGTC
Bcat1	TCGGGGAGTTGATAACAAGATCC	GGTCCTCACAGCAGATCGG
Bcat2	AAAGCATACAAAGGTGGAGACC	CGTAGAGGCTCGTTCCGTTG
Bckdha	CTCCTGTTGGGACGATCTGG	CATTGGGCTGGATGAACTCAA
Bckdhb	AGTGCCCTGGATAACTCATTAGC	GCATCGGAAGACTCCACCAAA
Acadsb	CCCAACCTGCTTGTCTCCTTG	ATCCCTGGATCACCGATTTCT
Pcca	TTCATACCAATGCCTAGTGGTGT	GACAGCCTCATCCGCCATTTT
Auh	AGCTGGCTCTAGCGTGTGA	GTTCTGTTCTAACACATGGCTGA
Hadhb	ACTACATCAAAATGGGCTCTCAG	AGCAGAAATGGAATGCGGACC
Glut1	CAGTTCGGCTATAACACTGGTG	GCCCCCGACAGAGAAGATG
Eno1	TGCGTCCACTGGCATCTAC	CAGAGCAGGCGCAATAGTTTTA
18s*	CGCTTCCTTACCTGGTTGAT	GAGCGACCAAAGGAACCATA
Rpl13a*	GGGCAGGTTCTGGTATTGGAT	GGCTCGGAAATGGTAGGGG
Gapdh*	AGGTCGGTGTGAACGGATTTG	TGTAGACCATGTAGTTGAGGTCA
β-actin*	GGCTGTATTCCCCTCCATCG	CCAGTTGGTAACAATGCCATGT
Rplp0*	AGATTCGGGATATGCTGTTGGC	TCGGGTCCTAGACCAGTGTTC
B2m*	TTCTGGTGCTTGTCTCACTGA	CAGTATGTTCGGCTTCCCATTC
Hprt*	TCAGTCAACGGGGGACATAAA	GGGGCTGTACTGCTTAACCAG
Pgk1*	ATGTCGCTTTCCAACAAGCTG	GCTCCATTGTCCAAGCAGAAT

* endogenous controls